PERGAMON

Quaternary International 83–85 (2001) 19–46

# Sea-level and environmental changes since the last interglacial in the Gulf of Carpentaria, Australia: an overview

Allan R. Chivas[a,*], Adriana García[a], Sander van der Kaars[b], Martine J.J. Couapel[a], Sabine Holt[a], Jessica M. Reeves[a], David J. Wheeler[a], Adam D. Switzer[a], Colin V. Murray-Wallace[a], Debabrata Banerjee[a,c], David M. Price[a], Sue X. Wang[a], Grant Pearson[a], N. Terry Edgar[d], Luc Beaufort[e], Patrick De Deckker[f], Ewan Lawson[g], C. Blaine Cecil[h]

[a] *School of Geosciences, University of Wollongong, Wollongong, NSW 2522, Australia*
[b] *School of Geography and Environmental Science, Monash University, VIC 3800, Australia*
[c] *Department of Physics, Oklahoma State University, Stillwater, OK 74078-3072, USA*
[d] *US Geological Survey, 600 4th Street South, St. Petersburg, FL 33701, USA*
[e] *Centre Européen de Recherche et d'Enseignement des Géosciences de l'Environnement (CNRS-CEREGE), BP 80, Aix-en-Provence, 13540 Cedex 4, France*
[f] *Department of Geology, The Australian National University, Canberra, ACT 0200, Australia*
[g] *Australian Nuclear Science and Technology Organisation (ANSTO), Lucas Heights Research Laboratories, PMB 1, Menai, NSW 2234, Australia*
[h] *US Geological Survey, MS-956, Reston, VA 20192, USA*

Accepted 29 May 2001

**Abstract**

The Gulf of Carpentaria is an epicontinental sea (maximum depth 70 m) between Australia and New Guinea, bordered to the east by Torres Strait (currently 12 m deep) and to the west by the Arafura Sill (53 m below present sea level). Throughout the Quaternary, during times of low sea-level, the Gulf was separated from the open waters of the Indian and Pacific Oceans, forming Lake Carpentaria, an isolation basin, perched above contemporaneous sea-level with outlet channels to the Arafura Sea. A preliminary interpretation is presented of the palaeoenvironments recorded in six sediment cores collected by the IMAGES program in the Gulf of Carpentaria. The longest core (approx. 15 m) spans the past 130 ka and includes a record of sea-level/lake-level changes, with particular complexity between 80 and 40 ka when sea-level repeatedly breached and withdrew from Gulf/Lake Carpentaria. Evidence from biotic remains (foraminifers, ostracods, pollen), sedimentology and geochemistry clearly identifies a final marine transgression at about 9.7 ka (radiocarbon years). Before this transgression, Lake Carpentaria was surrounded by grassland, was near full, and may have had a surface area approaching 600 km × 300 km and a depth of about 15 m. The earlier rise in sea-level which accompanied the Marine Isotopic Stage 6/5 transgression at about 130 ka is constrained by sedimentological and biotic evidence and dated by optical- and thermoluminescence and amino acid racemisation methods. 

## 1. Introduction

The Gulf of Carpentaria and adjacent Arafura Sea (Fig. 1) which today form a low-latitude epicontinental sea between Australia and the island of New Guinea, have fluctuated between open-ocean, estuarine, lacustrine, and subaerial exposure, during the sea-level changes of the Late Quaternary. Seismic evidence (in excess of 7000 line km) was collected in four cruises in 1982, 1993/94, 1995 (Arafura Sea) and 1997, and indicates a basin-wide late Neogene and Quaternary sedimentary sequence with repeated marine/non-marine cyclicity punctuated by numerous inferred exposure surfaces with deeply incised channels.

The modern epicontinental sea is shallow (maximum water depth 70 m) and thus in the past has registered global signatures of the major climatically-driven phases of marine transgression and regression. In addition, being located on a tectonically relatively stable portion

*Corresponding author.
*E-mail address:* toschi@uow.edu.au (A.R. Chivas).

1040-6182/01/$ - see front matter 
PII: S1040-6182(01)00029-5

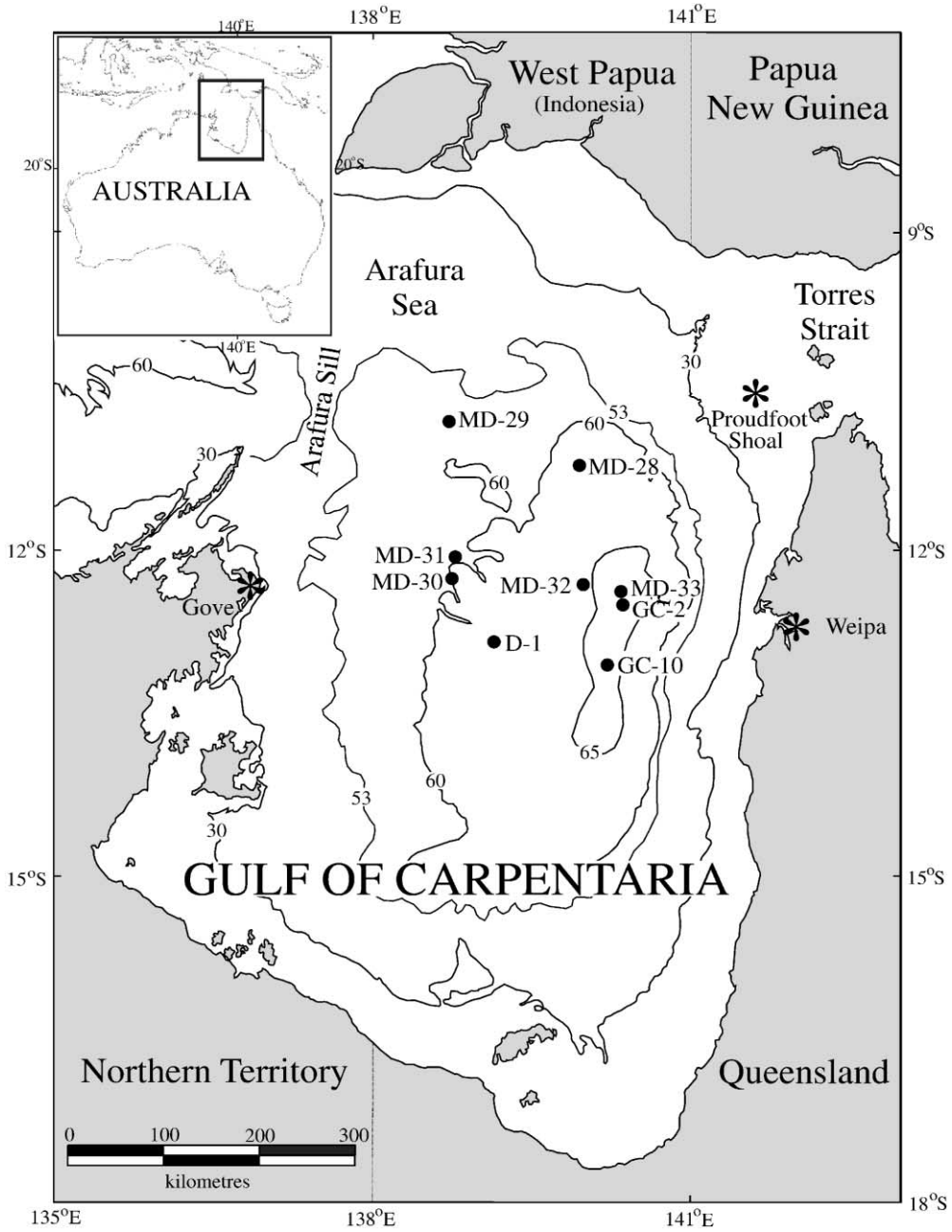


Fig. 1. Bathymetry of the Gulf of Carpentaria (from Grim and Edgar, 1998) and location of coring sites (MD- and GC- ). D-1 represents the location of the Duyken-1 well. The 53 m contour, represents the potential maximum size of Lake Carpentaria.

of the Australian plate, such a record of sea-level change can be more easily deciphered compared to areas that are affected by significant tectonic changes. The Gulf of Carpentaria is located in a significant tropical region of the world because it is adjacent to the Western Pacific Warm Pool which is responsible for the largest transfer of heat from the Pacific Ocean into the Indian Ocean and is implicated in the generation of El Niño/La Niña phases of the Southern Oscillation. A substantial transfer of moisture into the atmosphere is associated with this 'warm pool', and the Gulf region must have acted as a registry of atmospheric changes. Thus, a record of changes in the amount and seasonality of rainfall associated with each rise and fall of sea-level are probably recorded in the sediments, including the low-stand palaeosol exposure surfaces. Similarly, changes in the movement of the Intertropical Convergence Zone through time, and associated environmental effects, are expected to be found in the Gulf's long-term record. The region spans nearly ten degrees of latitude with

significant variation in modern rainfall from a two- to three-month winter dry season in the north to a six- to eight-month winter dry season in the south. There is the potential for the Gulf of Carpentaria to become a reference area for sea-level studies, tropical palaeoclimate (palaeomonsoons), and the linkage between marine and continental climatic records spanning the Quaternary and much of the Neogene.

## 2. Aims

This paper provides an introductory study of sediments from cores that span the past approximately 130 ka. The principal scientific objectives of coring the Gulf of Carpentaria include:

- Quaternary sedimentation processes and history, and sea-level changes.
- A history of ocean mixing between the Arafura and Coral Seas (i.e. the Indian and Pacific Oceans).
- Establishing past hydrological budgets and therefore a record of Quaternary palaeomonsoons in the Australia/Indonesia region (using palaeosols, palynomorphs, and the lacustrine sedimentary phases).
- Developing a model for the accumulation and preservation of organic matter in a tropical epicontinental sea as a modern analogue of ancient coal and hydrocarbon deposits (e.g. Cecil et al., 1985, 1993; Cobb and Cecil, 1993).
- Understanding the environmental tolerances of aquatic organisms in a large basinal system as it fluctuates between marine and non-marine conditions.
- Understanding the carbon cycle, including marine and non-marine carbonate production, in epicontinental seas.
- Understanding mixed carbonate and clastic systems as a function of climate and sea level (e.g. Cecil, 1990).

Several of these aims are addressed in this paper. Further assessment awaits the detailed micropalaeontological and geochemical work on foraminifers, ostracods, charophytes, coccoliths, dinoflagellates and diatoms which is in progress.

## 3. Background

### 3.1. The Carpentaria Basins

The deeper sedimentary units of the Gulf of Carpentaria form a series of stacked intracratonic basins and depressions (Smart et al., 1980; Passmore et al., 1993a, b) namely the Bamaga Basin (of possible Palaeozoic age), the Carpentaria Basin (Jurassic and Cretaceous), and the Karumba Basin (Neogene and Quaternary). There has been only a single deep drill hole sited in the central Gulf of Carpentaria, Duyken-1 (Fig. 1) by Canada Northwest Australia Oil N.L., which terminated at 1117 m, after intersecting Precambrian rhyodacite at 1113 m. Unfortunately, no cuttings or samples were recovered in the uppermost 210 m. Preliminary, widely spaced palynological observations have suggested the interval 210–405 m is of Miocene age; that the Cretaceous/Paleogene boundary is at about 550 m; with the interval 550–1110 m being largely of Middle and Early Albian age (Blake et al., 1984). The Bamaga Basin is located to the north-east of Duyken-1, and therefore, Palaeozoic and Jurassic rocks were not intersected.

The broad-scale tectonic and environmental evolution of these basins, with particular emphasis on the uppermost 300 m of sediments of probable Miocene to Pleistocene age, is provided by Edgar et al. (in press) using the results of a US Geological Survey high-resolution seismic survey conducted in 1993/1994 (Fig. 2). This survey (Edgar et al., 1994) delineated up to 17 reflectors, of which about 10 occur in the uppermost 150 m of the sedimentary succession and are marked by abundant incised channels, and erosional unconformities. This sequence has been interpreted to indicate at least 14, possibly 17, major transgressive/regressive events, within the 3 m resolution of the seismic system employed (Edgar et al., in press). These seismic data formed an important baseline for site selection during the 1997 IMAGES coring campaign described in this current paper.

### 3.2. Previous coring in the Gulf

Phipps (1966, 1970, 1980) recovered sediment cores up to 4 m in length, and noted marine sediments overlying non-marine strata, although the $^{14}C$ ages (bulk shells and/or bulked organic-matter; $\beta$-counting) from Phipps (1970) were not necessarily ascribed to appropriate facies. Phipps interpreted sediments that contained solely *Ammonia beccarii* as marine, whereas such sediments are now viewed as largely non-marine. Recently, Head et al. (1999) have shown from the $^{14}C$ activity of the bulk organic-carbon fraction in sediments from the Gulf of Carpentaria, that anomalously young carbon has penetrated to depths approaching 2 m. Accordingly, in this area, the application of $^{14}C$ dating is probably best restricted to carbonate materials.

During 1970 and 1972, shallow coring in the search for offshore bauxite occurred at distances up to 250 km west of Weipa by Canadian Superior Mining (Australia) Pty Ltd. Smart (1977) reviewed these data, noting the development of calcrete and iron-staining in sediments during periods of sub-aerial exposure, and confirming the widespread development of non-marine facies within an enclosed basin environment before 11 ka.

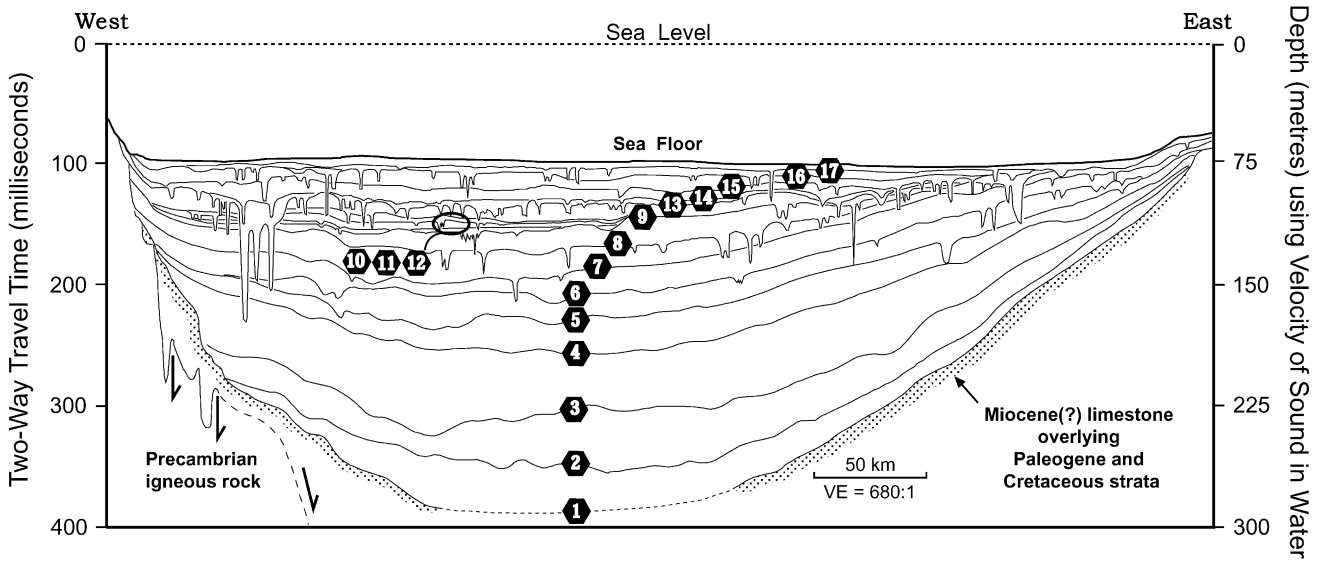


Fig. 2. Interpretative line-drawing of a seismic section (line 17 of USGS survey of 1993/94) across the Gulf of Carpentaria from Gove to Weipa (from Edgar et al., in press), showing numbered basin-wide reflectors and incised channels (width not to scale) at exposure surfaces.

A large co-operative seismic (1600 line km) and shallow-coring program (35 cores to about 2 m depth; 9 of which were examined in detail) in 1982 by Tom Torgersen (then at the Australian National University) and the Queensland Geological Survey (Mal Jones and others), left a wealth of data and is responsible for the current state of knowledge of the evolution of the Gulf during the past 40 ka. The resulting studies (Torgersen et al., 1983b, 1985, 1988; Jones and Torgersen, 1988) confirmed the former presence of 'Lake Carpentaria' (area 30,000–70,000 $km^2$), following the interpretation of Smart (1977) and Nix and Kalma (1972), and established the lake's hydrological balance during the past 40 ka at times when sea-level dropped below –53 m to expose the Arafura Sill (the 'Wessel Rise' of Fairbridge, 1953).

The 1982 cores were ideally suited for the development of new geochemical techniques because of the range of environments, from marine to lacustrine, available for investigation. Thus detailed geochemical and other studies (De Deckker et al., 1988, 1991; McCulloch et al., 1989; Norman and De Deckker, 1990; Vengosh et al., 1991), in particular, used Sr/Ca, Mg/Ca (Chivas et al., 1983, 1985, 1986a, b, 1993) and $^{87}Sr/^{86}Sr$ of ostracods and authigenic carbonates to define the chemistry of the lacustrine waters and sediments and the timing and heights of sea-level in breaching the Arafura Sill (−53 m) and Torres Strait Sill (−12 m). The location of two of the 1982 cores, GC-2 and GC-10A, which received most investigation are shown in Fig. 1, and referred to elsewhere in this paper.

A major ecological survey of the Gulf of Carpentaria in 1990 and 1991 by the CSIRO Division of Fisheries (Hill, 1994; Long and Poiner, 1994; and the following eleven papers), also provided a comprehensive two-dimensional survey of the modern sediments in the Gulf (Somers and Long, 1994; and coupled with Jones, 1987). These studies indicate the predominance of sand nearer the Gulf's eastern shore, with progressively increasing amounts of silt and mud in more central to northwestern sectors.

## 4. Results and interpretation

### 4.1. General stratigraphy of the 1997 cores

The materials available for the present paper, derive from an add-on cruise segment, partly financed by the Australian Research Council, as part of the IMAGES III (International MArine Global changE Study) program operated by the Institut Francais pour la Recherche et la Technologie Polaires (IFRTP). Six cores, from 4.2 to 14.8 m in length (Table 1, Fig. 1, and hereafter referred to in abbreviated form as MD-28–MD-33), were collected using a giant piston-core system deployed from the *Marion Dufresne* in June 1997 (Appendix A), during a short Australian/French/USA cruise from Cairns to the northern and central Gulf of Carpentaria then to the Gulf of Papua. Underway high-resolution seismic (800 Hz) data (to be presented elsewhere) were collected along direct transits between sites, and were used to select the core sites.

Table 1
Location and date of collection of sediment cores from the Gulf of Carpentaria[a]

| Core | Lat (°S) | Long (°E) | Water depth (m) | Total core depth (m) | Coring date and time |
|---|---|---|---|---|---|
| GC-2 | 12°31′ | 140°21′ | 67 | 2.2 | 1982 |
| GC-10A | 13°04′ | 140°12′ | 67 | 1.4 | 1982 |
| Duyken-1 | 12°53.001′ | 139°11.654′ | 59.2 | 1117 | 13–24 November 1984 |
| MD 972128 | 11°11.48′ | 139°57.53′ | 62 | 4.19 | 5 June 1997, 1213 h |
| MD 972129 | 10°47.36′ | 138°43.20′ | 60 | 6.24 | 5 June 1997, 2027 h |
| MD 972130 | 12°16.01′ | 138°44.92′ | 60 | 8.23 | 6 June 1997, 0521 h |
| MD 972131 | 12°03.96′ | 138°44.98′ | 59 | 13.60 | 6 June 1997, 0745 h |
| MD 972132 | 12°18.79′ | 139°58.73′ | 64 | 14.84 | 6 June 1997, 1457 h |
| MD 972133 | 12°23.55′ | 140°20.32′ | 68 | 6.58 | 6 June 1997, 1733 h |

[a] GC-2 and GC-10A data from Torgersen et al., 1988; Duyken-1 data from Blake et al., 1984.

The six cores were collected in water depths ranging from near the current bathymetric centre of the Gulf to shallower areas to the northwest (Fig. 1). The strategy was to provide a transect in current water depths of about 60–70 m that would intersect sediments deposited in Lake Carpentaria, across the former lake basin from depocentre to rim. This allows the direct estimation of lake palaeowater-depth, as core sites from nearer the basin margin will have been substantially exposed during periods of low lake-level. This supposition was immediately confirmed by the intense pedogenic overprint in basin-rim cores MD-28 and MD-29. Even cores MD-33 and MD-32 near the basin centre display pedogenesis in some intervals and therefore evidence for exposure of the lake floor.

An approximate west-east section from sites MD-30–MD-33 is shown in Fig. 3, with the more northerly cores, MD-28 and MD-29 projected onto the same section. This section is almost the same as the central portion of seismic line 17 in Fig. 2. Fig. 3 plots, at great vertical exaggeration, the position of the facies deposited during the most recent marine transgression, and of an older transgression (the latter in MD-32), dated to approximately 9.7 and 125 ka, respectively (see following section on dating methods). Also shown are the pedogenic intervals that consist of iron-mottling and soil-carbonate development. The lack of such sub-aerial exposure in the topmost 1 m of the upper non-marine facies is evidence for the presence of a substantial lake with water depth exceeding 10 m in the centre of the palaeolake. However, in core MD-28, a pedogenic interval is directly overlain by the most recent marine transgressive facies. Somewhat earlier, the lake was more restricted in area and depth (perhaps only 2–5 m deep) in the vicinity of MD-32 and MD-33, where the palaeosols occur at deeper stratigraphic levels. Unfortunately, we have insufficient dates to fully document the timing of these changes. The preliminary correlation between MD-31 and MD-32 (Fig. 3) is based upon the recognition of several marine/non-marine transitions (based on facies changes, and ostracod and foraminifer assemblages, observed at 10 cm intervals).

The detailed core logs (Figs. 4–9) show several parameters including the position (as a black side bar) of pedogenetically overprinted intervals, digital colour, *P*-wave velocity, bulk density, magnetic susceptibility and sediment particle size (Appendices B and C). In most cores, the poorly consolidated Holocene transgressive facies is readily discerned by its lower bulk density, higher water content and coarser particle-size, the latter probably largely owing to microfossil fragments. The older marine transgressive facies, below approximately 9.3 m in core MD-32 is less well indicated. Sediment particle-size, in general, in the deeper sections is not a clear indicator of environment. Although the basin-rim cores, MD-28 and MD-29, contain coarser sediment throughout than do basin-centre facies, this may be partly a pedogenic effect. The particle-size determinations for individual samples are incorporated in the lithological logs and most samples vary between clayey silt and silty clay. The pedogenic intervals are characterised by lower water contents, marginally higher magnetic susceptibility and higher bulk density, although bulk density is distinctly higher where soil carbonate nodules are abundant.

### 4.2. Dating

The successful dating of parts of the cores forms a crucial framework for understanding the development of the Gulf. Particularly significant are the results for the deeper sections, using amino acid racemisation (AAR) (Appendix D), thermoluminescence (TL) and optically-stimulated luminescence (OSL) (Appendix E) that permit initial correlation with the $\delta^{18}$O-derived sea-level curve.

#### 4.2.1. Radiocarbon

Torgersen et al. (1988) used twenty $^{14}$C ages ($\beta$-counting) of bulk carbonate and bulk shells from

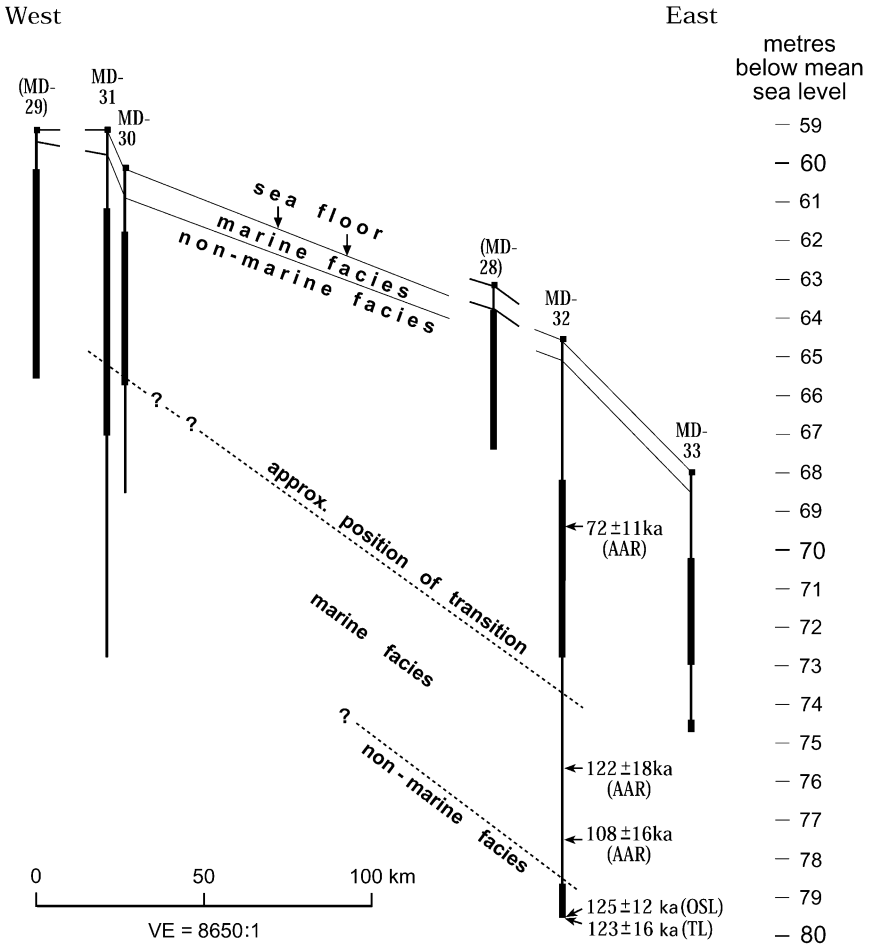


Fig. 3. West–east cross section within the Gulf of Carpentaria showing core locations. The wide black bars on each core location indicate the positions of pedogenic intervals. Note that the locations of MD-28 and MD-29 (Fig. 1), have been projected from more northerly positions. The core elevations were computed using the apparent water depth (±0.5 m) at the time of coring (Table 1), corrected by planar interpolation of the predicted tidal datums using information from Weipa, Proudfoot Shoal (10°32′S; 141°28′E) and Gove (the latter incorporates a half-hour time change), and their tidal-datums versus mean sea-level of 1.8, 2.7 and 1.6 m, respectively. The planar interpolation of tides during the coring of MD-28–MD-33 indicates tides, relative to mean sea-level, of −0.9, +1.0, −0.3, +0.1, −0.6 and −0.1 m, respectively. Accordingly, we have chosen to adjust the apparent water-column heights for MD-28 (from 62 to 63 m), MD-29 (from 60 to 59 m), and MD-32 (from 64 to 64.5 m). The tidal regime in the Gulf of Carpentaria is complex (e.g. Church and Forbes, 1981; Wolanski, 1993) and more detailed modelling may produce better estimates of tidal water-depths at the time of the 1997 coring.

sediments from 10 short cores to demonstrate the breaching of the Arafura Sill during rising sea-level about 12 ka BP, and establishment of fully marine conditions by about 8.5 ka BP. This corresponds to the change in sedimentation from lacustrine and brackish facies to open marine (greenish muds) at varying depths of 28–70 cm in cores MD-28–MD-33.

Accelerator mass spectrometer (AMS) $^{14}C$ methods have been applied to the MD cores to carefully reassess the previous radiocarbon ages because it is clear that a proportion of the calcareous fauna in the uppermost marine unit has been reworked from the underlying non-marine units, as indicated by the presence of abraded and overgrown non-marine ostracods (e.g. *Ilyocypris* and *Cyprideis*). Furthermore, the Sr/Ca ratios of most but not all of the individual *Cyprideis* valves in the marine section of core GC-2, clearly indicate their reworking (De Deckker et al., 1988 Fig. 2). The new radiocarbon ages (Table 2) were undertaken at the ANSTO AMS Centre and were determined for small molluscs (one to three, per sample) and ostracods. The samples chosen were well preserved, clean and without evidence for reworking. The *Paranesidea* (ostracod) sample from MD-28 at 15–16 cm depth, was selected (rather than *Cyprideis*, at the same interval) as a truly marine species, to avoid the possible reworking noted above. The ages are plotted in stratigraphic position on the logs of Figs. 4–9.

Though further radiocarbon dating is in progress, the fairly complete data for core MD-28 indicate a fairly uniform deposition rate above a depth of 66 cm at 14 kaBP (based on five radiocarbon ages). The limited data for the other MD cores support the same general sedimentation rate, with the deepest sample being at

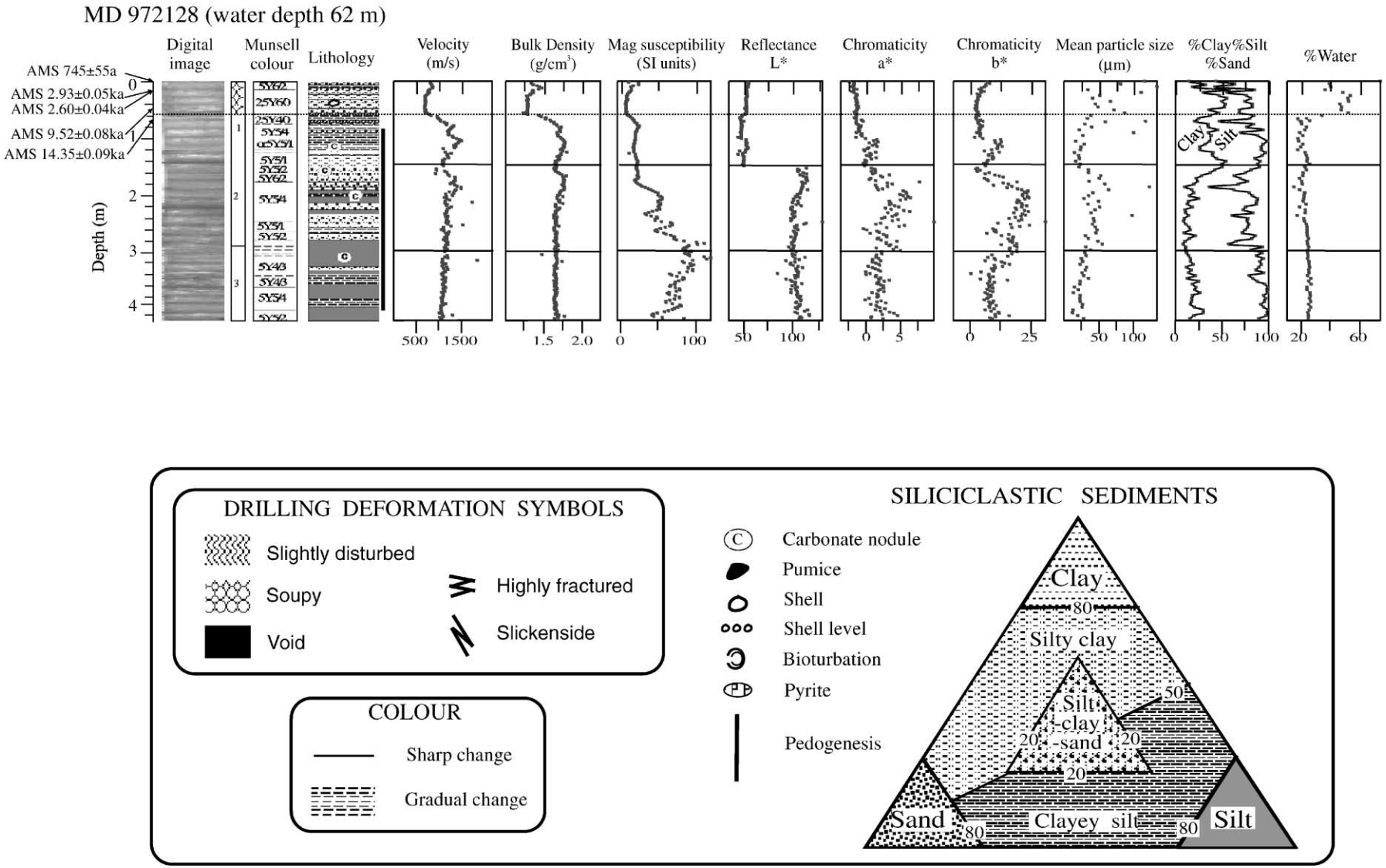


Fig. 4. Lithologic and physical-properties log of core MD-28. The information on colour includes reflectance (lightness variable, $L^*$) and chromaticity (wavelength bands, $a^*$ and $b^*$) as determined on-board using a Minolta Spectrophotometer CM-2002. $L^*$ corresponds to the weighted sum of the spectral reflectance of the specimen divided by that of a perfect reflecting diffuser. $L^*$ is therefore a unitless ratio. *P*-wave velocity, bulk density (from gamma-ray attenuation), and magnetic susceptibility measurements (all at 2 cm intervals) are from the ship-board multi-sensor track (MST) scanner. Particle-size analysis (mean particle-size and clay/silt/sand percentages) and water contents (at 5 cm intervals) were measured at the University of Wollongong. The dotted horizontal lines in the upper metre of each core (Figs. 4–9) mark the position of the non-marine/marine transition. The grey-scale digital image has been converted from an original digital colour image and the prominent banding at 20–50 cm intervals represents image frame-boundaries. The lithology column is based on the grain-size analysis and the triangular clay-silt-sand fields for siliciclastic sediments. The position of dated samples from within each core are labelled by technique and age, with AMS = $^{14}$C by Accelerator Mass Spectrometry (conventional radiocarbon years before present, Table 2); AAR = Amino Acid Racemisation; OSL = Optically Stimulated Luminescence, TL = Thermoluminesence.

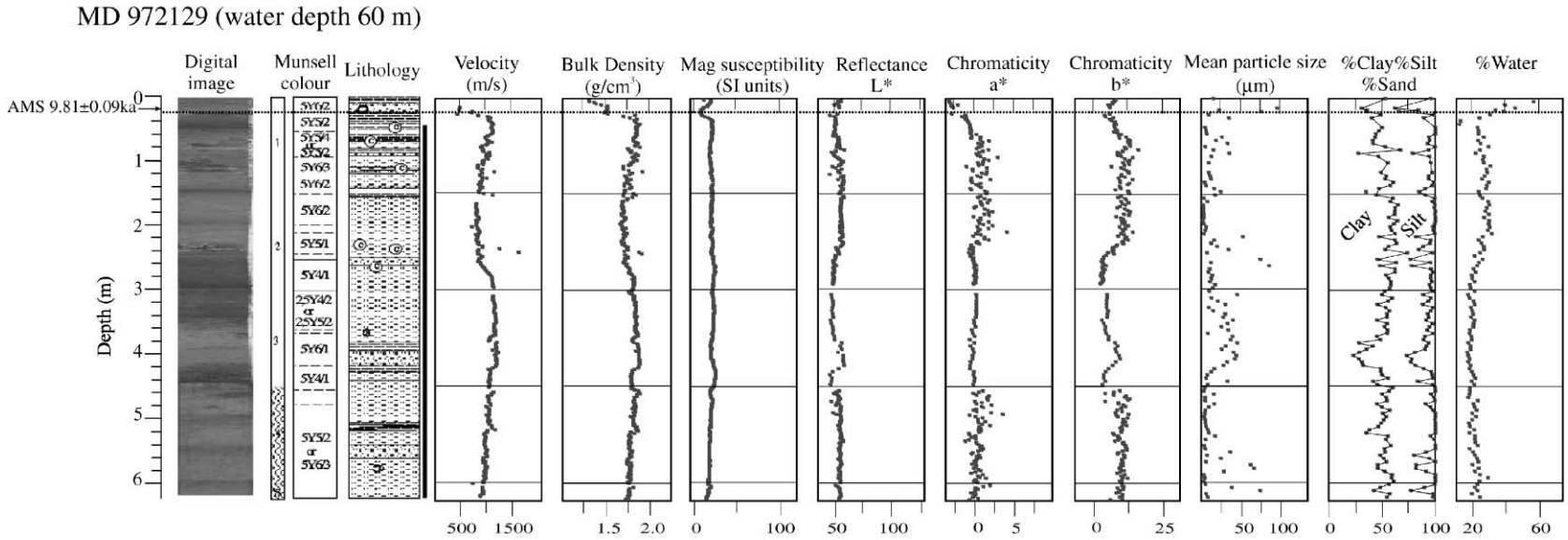


Fig. 5. Lithologic and physical-properties log of core MD-29 (see Fig. 4 caption for further explanation).

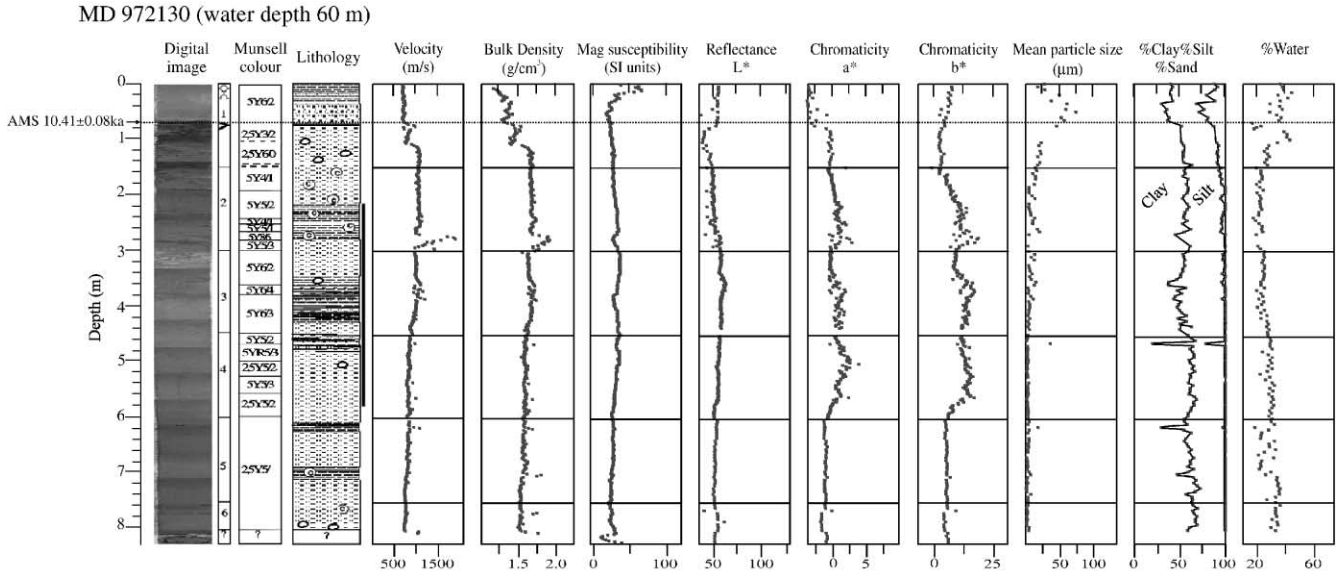


Fig. 6. Lithologic and physical-properties log of core MD-30 (see Fig. 4 caption for further explanation).

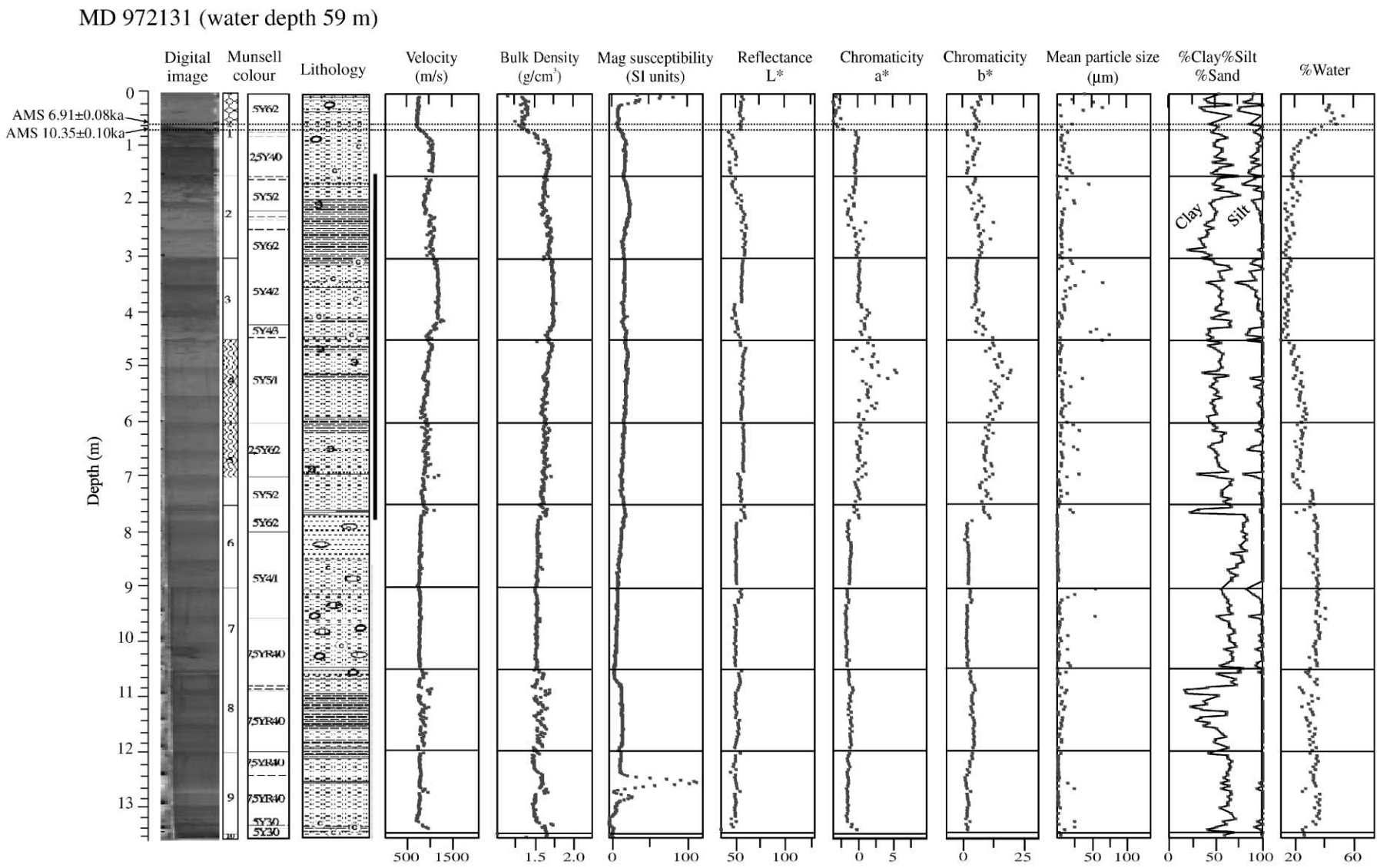


Fig. 7. Lithologic and physical-properties log of core MD-31 (see Fig. 4 caption for further explanation).

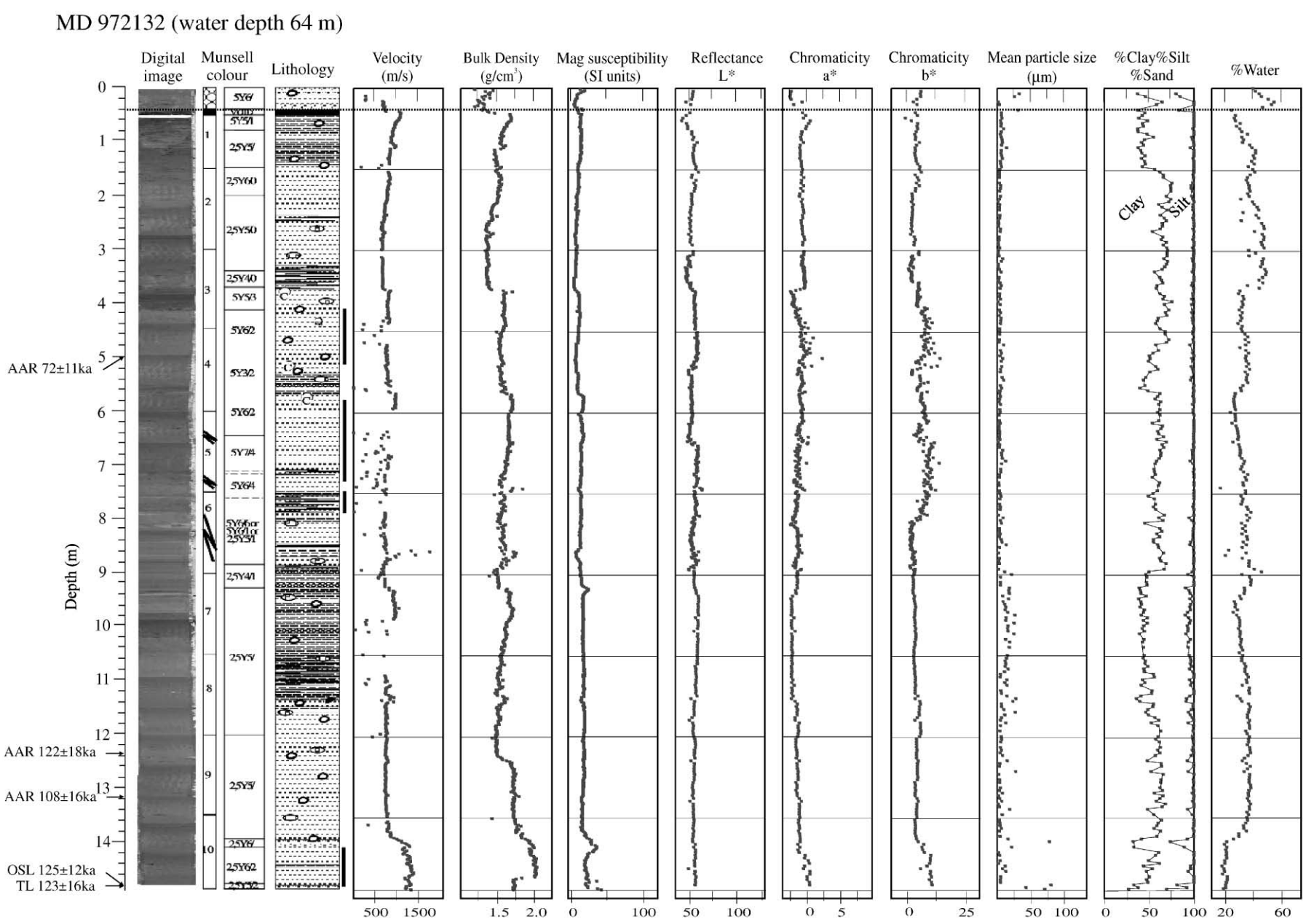


Fig. 8. Lithologic and physical-properties log of core MD-32 (see Fig. 4 caption for further explanation).

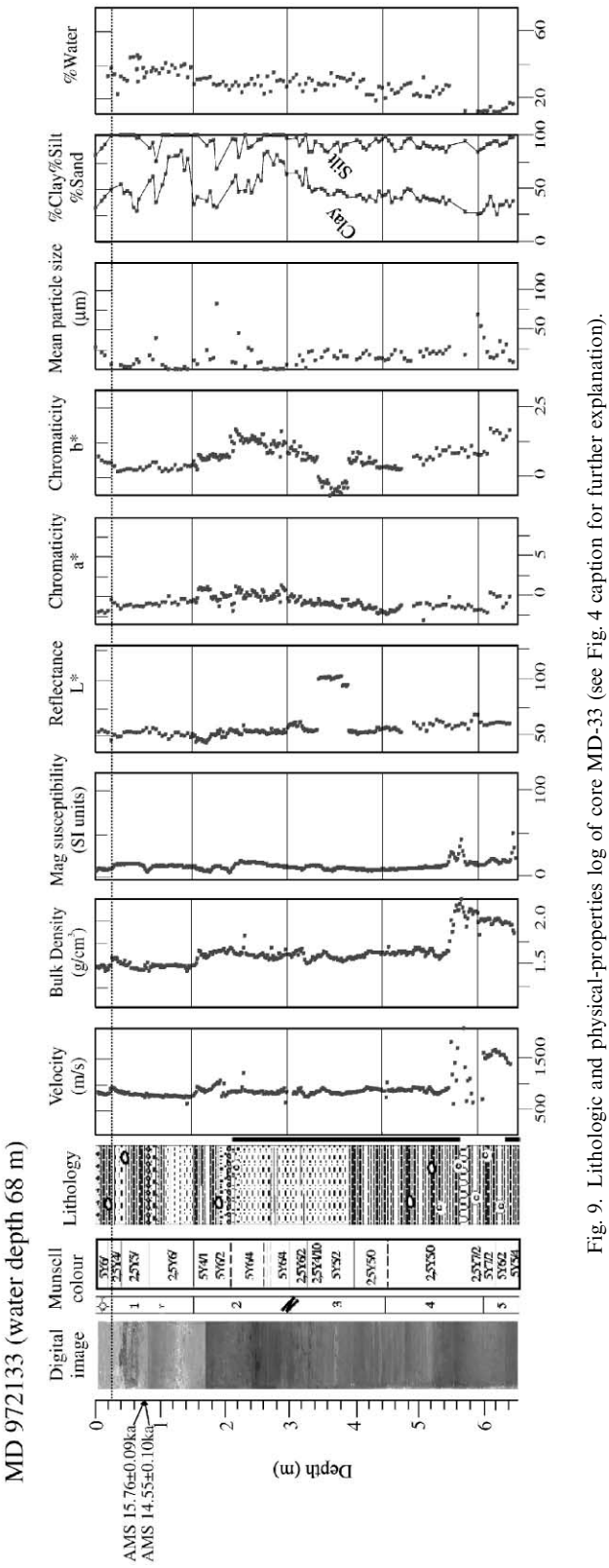


Fig. 9. Lithologic and physical-properties log of core MD-33 (see Fig. 4 caption for further explanation).

77–78 cm in MD-33 (approx 15 ka BP). Where replicated, there is fair correspondence between the $^{14}C$ ages on ostracods and molluscs from the same interval (MD-28 15–16 cm, and MD-33 77–78 cm).

Those samples from above the transition to fully marine conditions yielded conventional radiocarbon ages of $9520 \pm 80$ a (MD-28) and $6910 \pm 80$ a (MD-31). Radiocarbon ages in the upper levels of the underlying non-marine facies are $14{,}350 \pm 90$ a (MD-28), $9810 \pm 90$ a (MD-29), $10{,}410 \pm 80$ a (MD-30), and $10{,}350 \pm 90$ a (MD-31). The simplest interpretation is that the marine transgression occurred at about 9700 a BP, a result not that different from the previous estimate of approximately 8500 a BP for this same transition (Torgersen et al., 1988, for core GC-2). Additional samples are currently being analysed to investigate whether this diachroneity can be resolved.

### 4.2.2. *Amino acid racemisation dating*

AAR analyses (total acid hydrolysate) were undertaken on the fossil marine molluscs *Anadara* (*Tegillarca*) *granosa* and *Bassina* sp., from three levels in core MD-32, following the methods (Appendix D) documented in Murray-Wallace (1993). Preliminary ages (Table 3), their uncertainties, and the assumptions made in calibrating their numeric ages are outlined in Appendix D. These results are also plotted on Figs. 3 and 8, and indicate ages up to approximately 120 ka near the base of core MD-32 at core depths of 12.4–13.2 m.

### 4.2.3. *Luminescence dating*

To supplement the radiocarbon dating and AAR chronology, we utilised OSL, which has proven successful in lacustrine sediments containing quartz grains, and also TL dating (Appendix E). A sandy sample near the base of core MD-32 at 1482–1483 cm was chosen.

For this sample, the average value of the ratio of the fourth to first sensitivity-corrected regeneration dose OSL signal is $0.97 \pm 0.07$ (thirteen independent measurements; $n = 13$). This shows that the sensitivity correction is reliably correcting for any changes in the luminescence efficiency (or sensitivity) of the sample which might have occurred during the various regeneration cycles. A OSL growth curve for the sample is shown in Fig. 10. It can be seen that the sensitivity-corrected regeneration OSL signal keeps increasing at doses well beyond the dose corresponding to the natural signal. Thus, it is feasible to provide a reliable equivalent dose estimate for this sample. The mean equivalent dose estimate for the sample is $246 \pm 15$ Gy ($n = 13$). The dose-rate estimate of 1.96 mGy $a^{-1}$ provides a preliminary OSL age of $125 \pm 12$ ka for the sample. Interestingly, the TL age for this sample is $123 \pm 16$ ka. It is noteworthy that the OSL and TL ages have been determined using two different luminescence signals with

Table 2
AMS radiocarbon ages from carbonate microfossils from the Gulf of Carpentaria. The ages are initially presented in conventional radiocarbon years (5730 a half-life), corrected for isotopic fractionation, and without reservoir correction[a,b]

| Core and depth (cm) | ANSTO No. | Material and weight of $CaCO_3$ | $\delta^{13}C_{V-PDB}$ (‰) | Conventional $^{14}C$ age (a BP) $\pm 1\sigma$ | Calibrated $^{14}C$ age (a BP) |
|---|---|---|---|---|---|
| MD-28 0–1 | OZE263 | Three mollusc valves (7.8 mg) | 0 | 745 ± 55 | 410 |
| MD-28 15–16 | OZE260 | *Paranesidea* (60 ostracod valves; 1.4 mg) | 0 | 2930 ± 50 | 2720 |
| MD-28 15–16 | OZE261 | Three mollusc valves (7.5 mg) | +1.44 | 2600 ± 40 | 2300 |
| MD-28 50–51 | OZE257 | Single mollusc valve (8.4 mg) | −2.19 | 9520 ± 80 | 10,280 |
| MD-28 66–67 | OZE254 | Five mollusc valves (7.2 mg) | 0 | 14,350 ± 90 | 16,880 |
| MD-29 20–21 | OZE259 | Single mollusc valve (18.9 mg) | +0.16 | 9810 ± 90 | 11,200 |
| MD-30 70–71 | OZE250 | Four mollusc fragments (1.6 mg) | 0 | 10,410 ± 80 | 12,094 |
| MD-31 55–56 | OZE256 | Mollusc fragment (14.2 mg) | −0.18 | 6910 ± 80 | 7420 |
| MD-31 65–66 | OZE251 | Two mollusc fragments (1.2 mg) | 0 | 10,350 ± 100 | 12,020 |
| MD-33 77–78 | OZE252 | *Cyprideis* (135 ostracod valves; 5.2 mg) | 0 | 15,760 ± 90 | 18,570 |
| MD-33 77–78 | OZE253 | Two mollusc valves (8.1 mg) | −1.82 | 14,550 ± 100 | 17,120 |

[a] Samples with $\delta^{13}C$ values shown as 0‰ produced insufficient $CO_2$ to prepare an aliquot for $^{13}C$ determination. The $\delta^{13}C$ value of 0 is assumed for these samples. An error in $\delta^{13}C$ of 1‰ corresponds to an error of 8 radiocarbon years.

[b] The calibrated $^{14}C$ ages (an approximate calendar timescale, pre-1950 AD) were calculated using the relationships provided by Stuiver and Reimer (1993), for samples with conventional ages less than 10 ka; and using Bard et al. (1998), for samples older than 10ka. For marine samples a reservoir correction of 400 years has been applied. No reservoir correction is applied for lacustrine samples (OZE 254, 259, 250, 251, 252, 253) because of the current absence of information concerning lacustrine $^{14}C$ reservoir values for Lake Carpentaria.

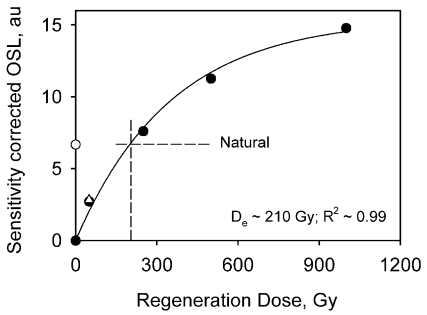


Fig. 10. Sensitivity-corrected OSL growth curve for an aliquot of quartz from sample MD-32, 1482 cm. The corrected natural OSL is shown as an unfilled circle, and the first four regeneration signals as filled circles. The fifth regeneration dose signal is shown as an unfilled triangle. A single saturating-exponential curve has been used to fit the regeneration OSL data.

different stimulation efficiencies, and for two different grain-size fractions.

However, a common source of uncertainty in both TL and OSL ages is the possibility of disequilibrium in the $^{238}U$ series. Radioactive disequilibrium has been previously observed in deep-sea sediments (Wintle and Huntley, 1979). The continuous precipitation of $^{230}Th$ and $^{231}Pa$ from the ocean and subsequent incorporation into sediments can result in radioactive disequilibrium and a time-dependent dose-rate in the sediment. Thus, additional radioactivity measurements (high-resolution $\gamma$-spectrometry, NAA and DNAA) are necessary to confirm the dose-rate estimate and the luminescence ages for the sample from MD-32 at 1482 cm.

### 4.3. Foraminifera, Ostracoda and Charophyta

The boundary between non-marine and marine facies, at 58.5 cm in MD-28 and at 59.5–68 cm in MD-31, is strikingly delineated by the microfossil assemblages. The uppermost marine sediments have a similar assemblage of microfossils in both cores (see Appendix G for preparation methods). About 120 species of foraminifers were recognised, though only 24 species are represented at more than 2% abundance, the minimum percentage used for the graphs (Fig. 11). The marine ostracods are represented by more than 30 species. Yassini et al. (1993), reported 82 ostracod species in a wider sampling of modern environments, with emphasis on littoral areas of the Gulf of Carpentaria. The species diversity found in the marine unit clearly contrasts with the diversity registered in the underlying non-marine unit, where typically only one species of foraminifer is present, together with up to 5 species of ostracod and one species of charophyte. The marine sediments show greater diversity and a lower number of individuals of each species, whereas the non-marine samples show less diversity but a much greater number of individuals of each taxon.

An open marine, shallow-water environment is indicated for the uppermost unit from both cores (Fig. 11). Foraminifers are mainly represented by benthic species, with 23 species with abundance greater than 2%, while only one species of planktic Foraminifera, *Gallitellia vivans*, a small taxon of less than 150 μm in length, is well represented. Among the benthic species, the more abundant taxa are *Textularia secasensis*, *Textularia* sp., *Ammomassilina alveoliniformis*,

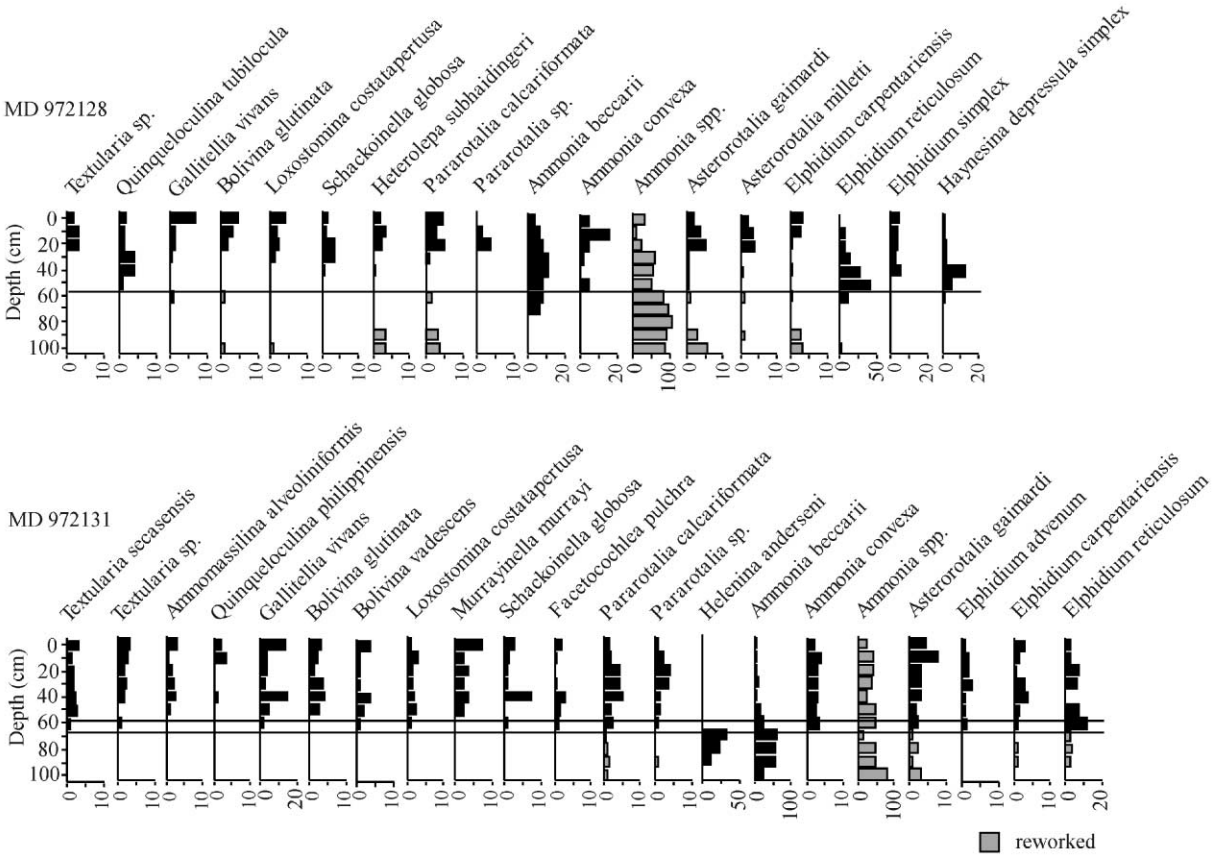


Fig. 11. Foraminiferal assemblages (species relative abundance, %) of the top metre of cores MD-28 and MD-31. Samples are 1 cm thick and at 10 cm intervals; the depth-increment interval of the diagrammatic bars is exaggerated in thickness. The horizontal lines mark the position of the non-marine/marine transition.

*Quinqueloculina philippinensis*, *Q. tubilocula*, *Bolivina vadescens*, *B. glutinata*, *Loxostomina costatapertusa*, *Facetocochlea pulchra*, *Heterolepa subhaidingeri*, *Murrayinella murrayi*, *Schackoinella globosa*, *Elphidium advenum*, *E. carpentariensis*, *E. reticulosum*, *E. simplex*, *Haynesina depressula simplex*, *Ammonia convexa*, *A. beccarii*, *Helenina anderseni*, *Asterorotalia gaimardi*, *A. milletti*, *Pararotalia calcariformata* and *Pararotalia* sp. There is a large number of specimens of reworked *Ammonia* spp. which constitute between 5–45% of the total specimens. Other taxa with representation a little less than 2% are*:* *Clavulina pacifica*, *Triloculina* sp., *Pyrgo* sp., *Globigerina bulloides*, *Cibicides floridanus*, *Lobatula lobatula*, *Rosalina* sp., *Cancris* sp., *Fissurina crassiporosa*, *Lagena dorbignyi*, *Lachlanella compressiostomata*, *Pseudorotalia angusta* and *Procerolagena* sp.

The ostracods in this uppermost marine unit are represented by *Cytherella semitalis*, *C. darwinensis carpentariana*, *Cytherelloidea malaccaensis*, *Paranesidea onslowensis*, *Neonesidea australis*, *Pseudopsammocythere* sp., *Callistocythere warnei*, *Labutisella* sp., *Keijia* sp., *Hemicytheridea* sp., *Paijenborchella solitaria*, *Venericythere papuensis*, *Pistocythereis cribriformis*, *Actinocythereis* sp., *Pterygocythereis velivola*, *Neocytheretta adunca*, *N. spongiosa*, *Cytherura* sp., *Semicytherura* sp., *Cytheropteron wrighti*. There is also an abundance of reworked non-marine taxa such as *Cyprideis australiensis* and *Ilyocypris australiensis*.

The main differences between cores MD-28 and MD-31 lie in the biological content of their non-marine sections. Core MD-28, located in the northern part of the Gulf of Carpentaria, has an assemblage between 60 and 90 cm of *Ammonia* spp., with a very high proportion of reworked specimens, and *Cyprideis australiensis*, indicative of non-marine, saline conditions, typical of saline inland lakes, coastal lagoons or an open estuary. At 90–100 cm depth, some reworked marine taxa are added to the previous assemblage (*Heterolepa subhaidingeri*, *Asterorotalia gaimardi*, *A. milletti*, *Pararotalia calcariformata*, *Elphidium carpentariensis*), probably from an underlying marine facies or an upslope marine unit which was exposed and eroded.

In core MD-31 the non-marine facies is represented at 70–80 cm depth by mainly small specimens of *Ammonia* spp., *Helenina anderseni*, with several specimens of the latter showing evidence of transport, and *Cyprideis*

*australiensis*, *Ilyocypris australiensis*, *Darwinula* sp., and the charophyte *Chara zeylanica*, indicative of freshwater conditions. At 90–100 cm depth some taxa from shallow-marine environments appear, most of them reworked, probably from a previous marine cycle or an upslope marine unit (*Elphidium carpentariensis*, *E. reticulosum*, *Asterorotalia gaimardi*, *A. milletti*, *Pararotalia calcariformata*, *Pararotalia* sp.).

### 4.4. Palynology

The vegetation history recorded in the uppermost 1.5 m of two cores (MD-28 and MD-29) from the north of the modern Carpentaria basin, and of three cores (MD-30, MD-31 and MD-33) from the west-central and east-central area has been investigated at 5 cm intervals (Appendix G, Figs. 12–16).

The most striking feature in all four cores is the boundary between the marine (Zone 1) and non-marine sedimentary facies (Zones 2–4), that is also independently delineated by palynological assemblages. Zone 1 is characterised by transported woodland, lowland and montane taxa, mangrove pollen and pteridophytes, as well as the dominant taxa related to swamp and grassland. The various non-marine zones below Zone 1 show an abundance of local swamp and grassland taxa and, in some zones, *Botryococcus*, *Typha* and *Pediastrum*. Based on the abundances of various taxa, the following preliminary environmental interpretations are offered. A more detailed discussion will be presented elsewhere.

*MD-28 Zone 2*. A possible low-lake phase; grasses and *Typha* in and around a shallow lake with aquatic ferns and *Botryococcus*. Zone 3 may represent a still lower lake level with grasses and *Typha*, aquatic ferns and some *Botryococcus*. The low representation of Chenopods may be an indication of relatively fresh water during deposition of these two zones.

*MD-29 Zone 2*. This zone may represent a swampy phase with grasses and sedges growing on swampy soil with *Anthoceros* and very few aquatic ferns and *Botryococcus* and a low abundance of Chenopods.

*MD-30 Zone 2*. A possible freshwater lake phase with grasses, sedges and *Pediastrum*. Zone 3 is a possible low-lake phase with grasses and sedges in and around a shallow lake with aquatic ferns (*Ceratopteris*). Zone 4 represents a swampy phase with grasses and saltbush (Chenopodiaceae) on swampy, possible saline, soil.

*MD-31 Zone 2*. A shallow lake phase with grasses, sedges and *Zygnema* in and around a very shallow lake. Zone 3 probably represents a slightly deeper lake phase with *Pediastrum*, while Zone 4 again reflects very shallow lake conditions, with mostly grasses and some sedge and *Zygnema*.

*MD-33 Zone 2*. This zone represents a shallow lake phase with sedges and grasses in and around a lake with some *Botryococcus*, *Pediastrum* and *Typha*. Zone 3 is a lake with *Casuarina*, grasses, sedges and *Typha* around a lake with *Botryococcus*, *Pediastrum* and some *Coelastrum*. The Zone 4 lake had *Callitris*, sedges and grasses around a lake with *Botryococcus*, *Coelastrum* and *Pediastrum*. The lake may have been progressively deepening.

In summary, the local vegetation during the non-marine phase largely consisted of open grasslands and swamps with sedges and very shallow lakes in the western part of the Carpentaria region (MD-29, MD-30, MD-31) while swamps with grasses, sedges and *Typha* and somewhat deeper lake conditions seem to have prevailed in the eastern part (MD-28, MD-33).

### 4.5. Carbon and nitrogen geochemistry

The nature of the transition from non-marine to marine facies in the upper metre of all six MD cores has been investigated using several geochemical parameters, namely $CaCO_3$ content, organic carbon and organic nitrogen contents, atomic C/N ratios, and the carbon-isotope ratio of the total organic carbon fraction (Appendix H, Fig. 17).

The position of the 9700 a BP marine transgression in each core as marked in Fig. 17 is based on the abrupt visual facies change. Not surprisingly, water content (Figs. 4–9) and carbonate content (Fig. 17) also delineate this transition, as the marine material has more abundant calcareous fossils. In cores MD-30 and MD-31, the organic carbon content is clearly higher in the non-marine facies, but in the other cores the organic carbon contents (about 0.4% C) of both facies are similar, although much lower (0.1–0.2% C) in cores MD-28 and MD-29 which display evidence of pedogenesis. The C/N ratios in the non-marine facies of cores MD-30 and MD-31 are higher than in their marine sections, although such a distinction does not occur in the other cores. The Holocene transgressive boundary in core MD-31 occurs as an angular unconformity dipping at about 40° over the interval from 59.5 to 68.0 cm. Paired samples from the two facies were analysed from four 1 cm vertical intervals at this contact and these are represented by overlapping curves for several parameters for this core (Fig. 17).

Rothlisberg et al. (1994) present $\delta^{13}C$ values of modern particulate organic matter from chlorophyll-maximum water depths across the Gulf of Carpentaria. In the vicinity of the MD coring sites, such particulate matter has $\delta^{13}C$ values of about –18 to –22.5‰ versus V-PDB, and contains phospholipid-derived fatty acids indicative of a marine phytoplankton source, with little evidence of terrestrial organic carbon sources. Elsewhere in northern Australia and New Guinea, the $\delta^{13}C$ values of recently deposited bulk organic marine carbon is in the range –19 to –20‰ (Van Dieman Gulf, Northern

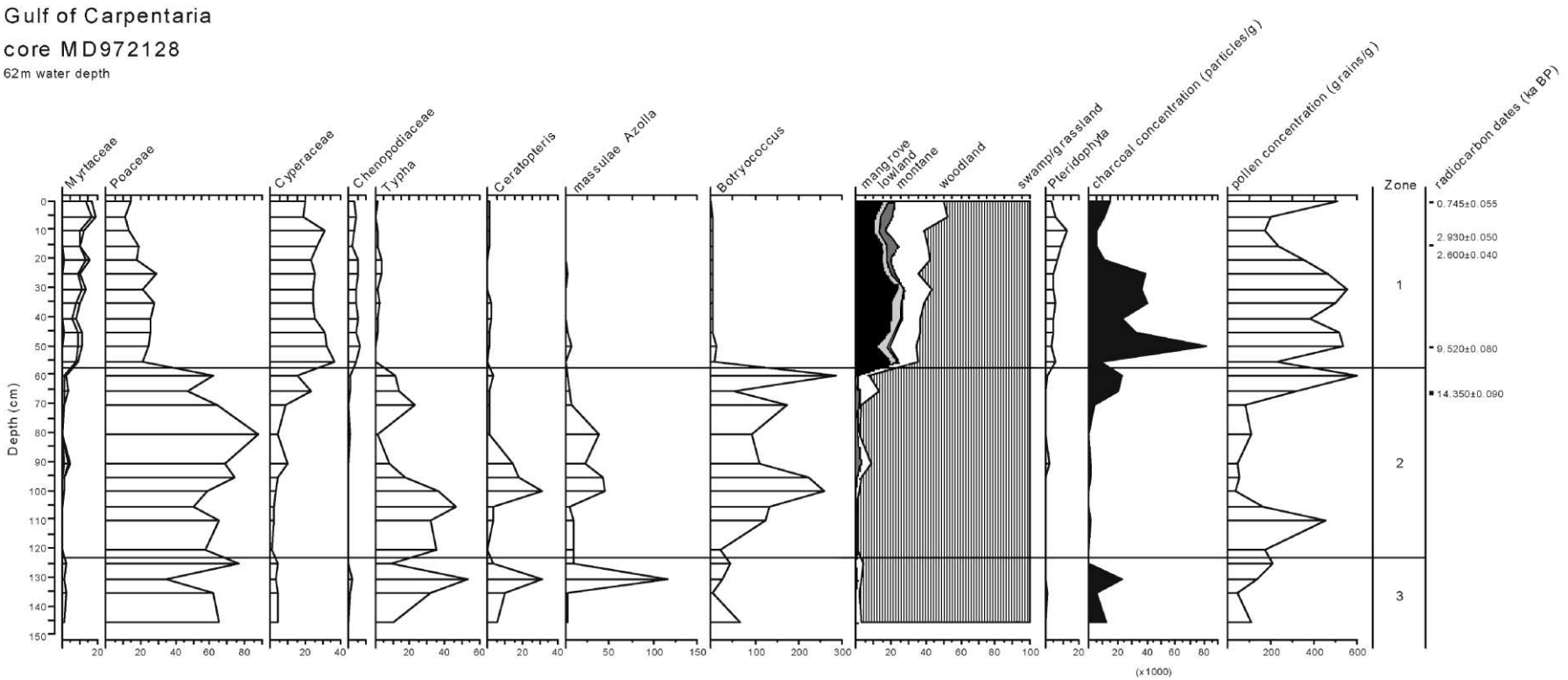


Fig. 12. Summary pollen diagram for the upper 150 cm of core MD-28 from the Gulf of Carpentaria. (Dates at right are expressed in conventional radiocarbon years; Table 2).

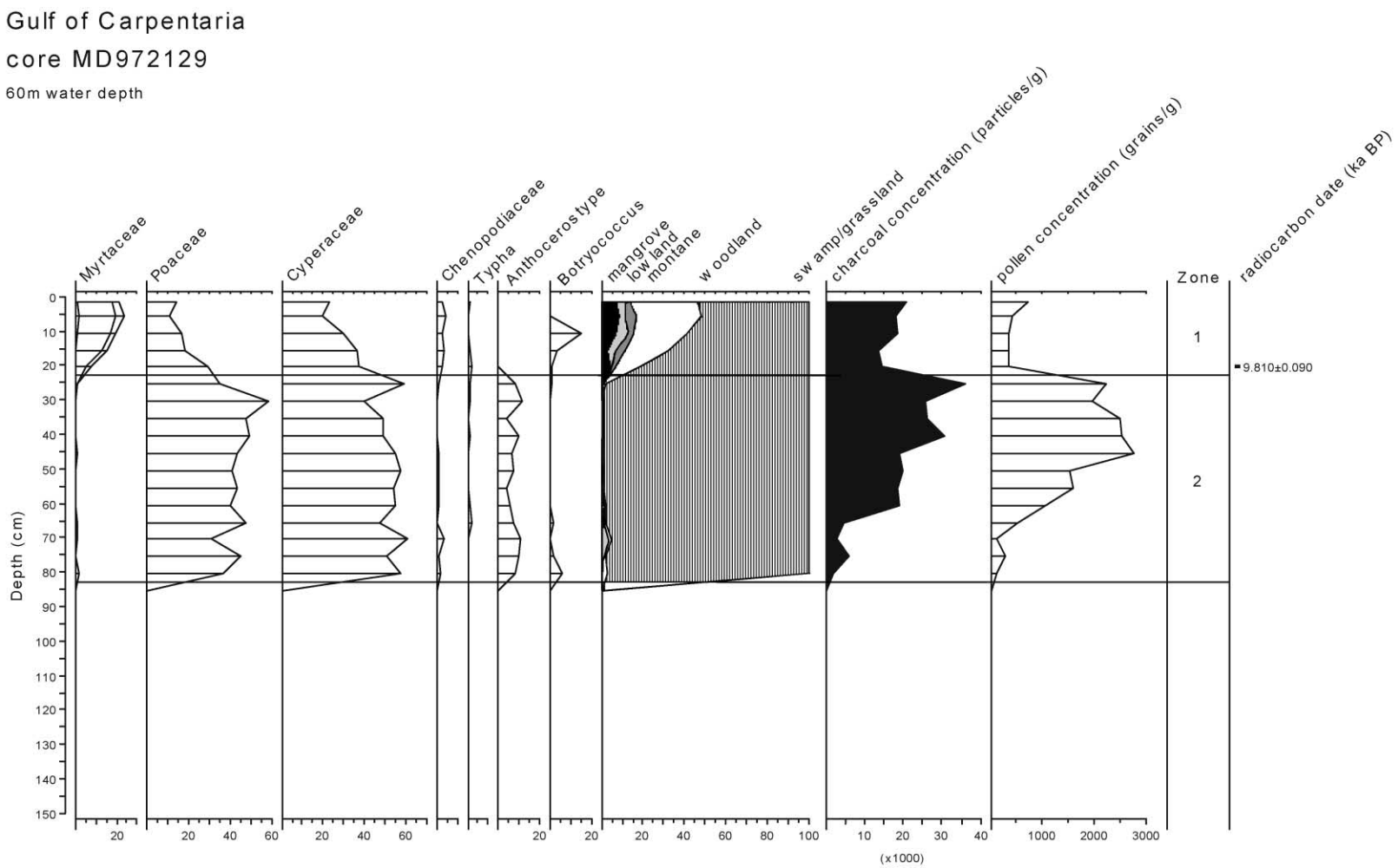


Fig. 13. Summary pollen diagram for the upper 150 cm of core MD-29 from the Gulf of Carpentaria.

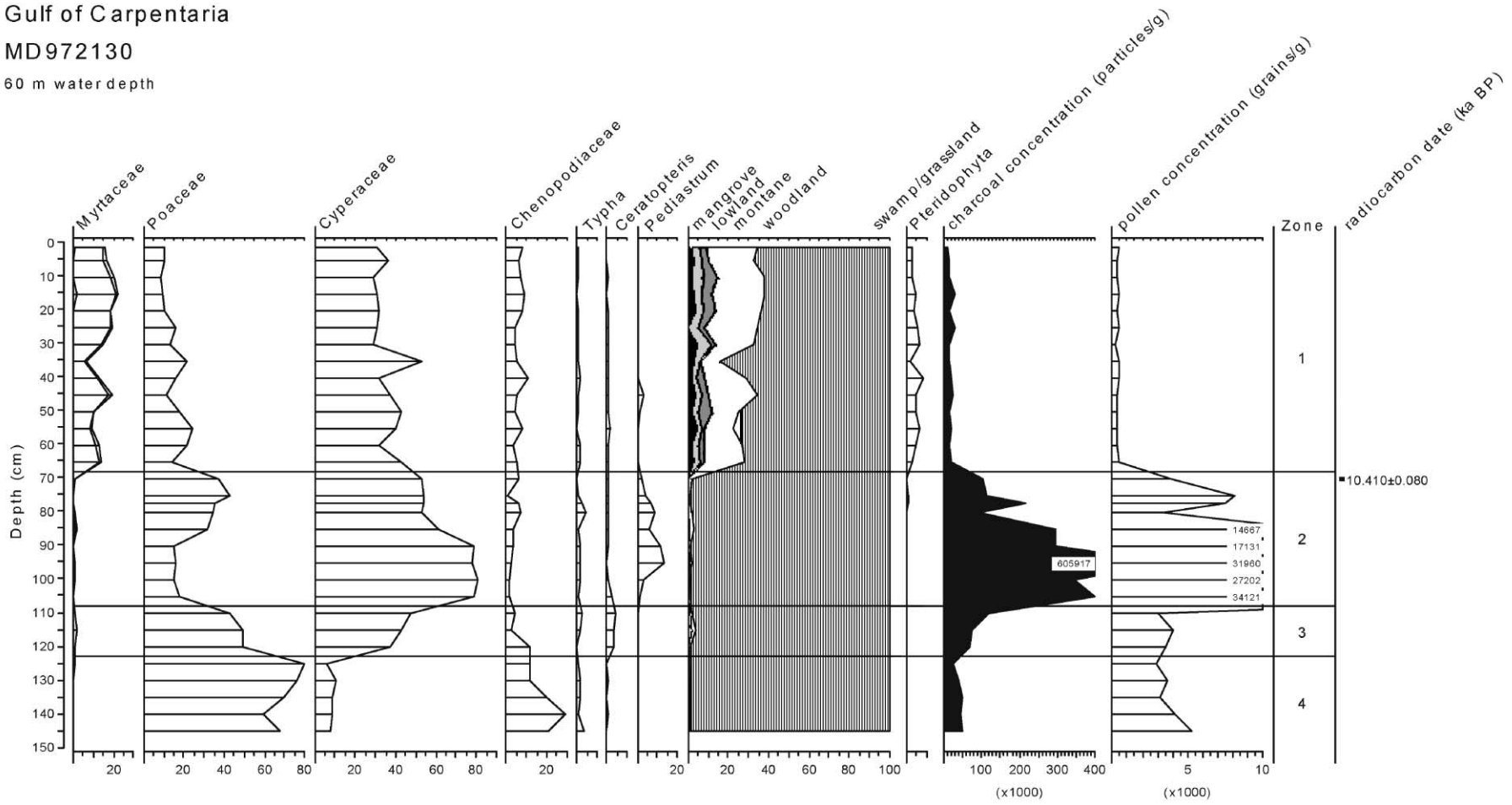


Fig. 14. Summary pollen diagram for the upper 150 cm of core MD-30 from the Gulf of Carpentaria.

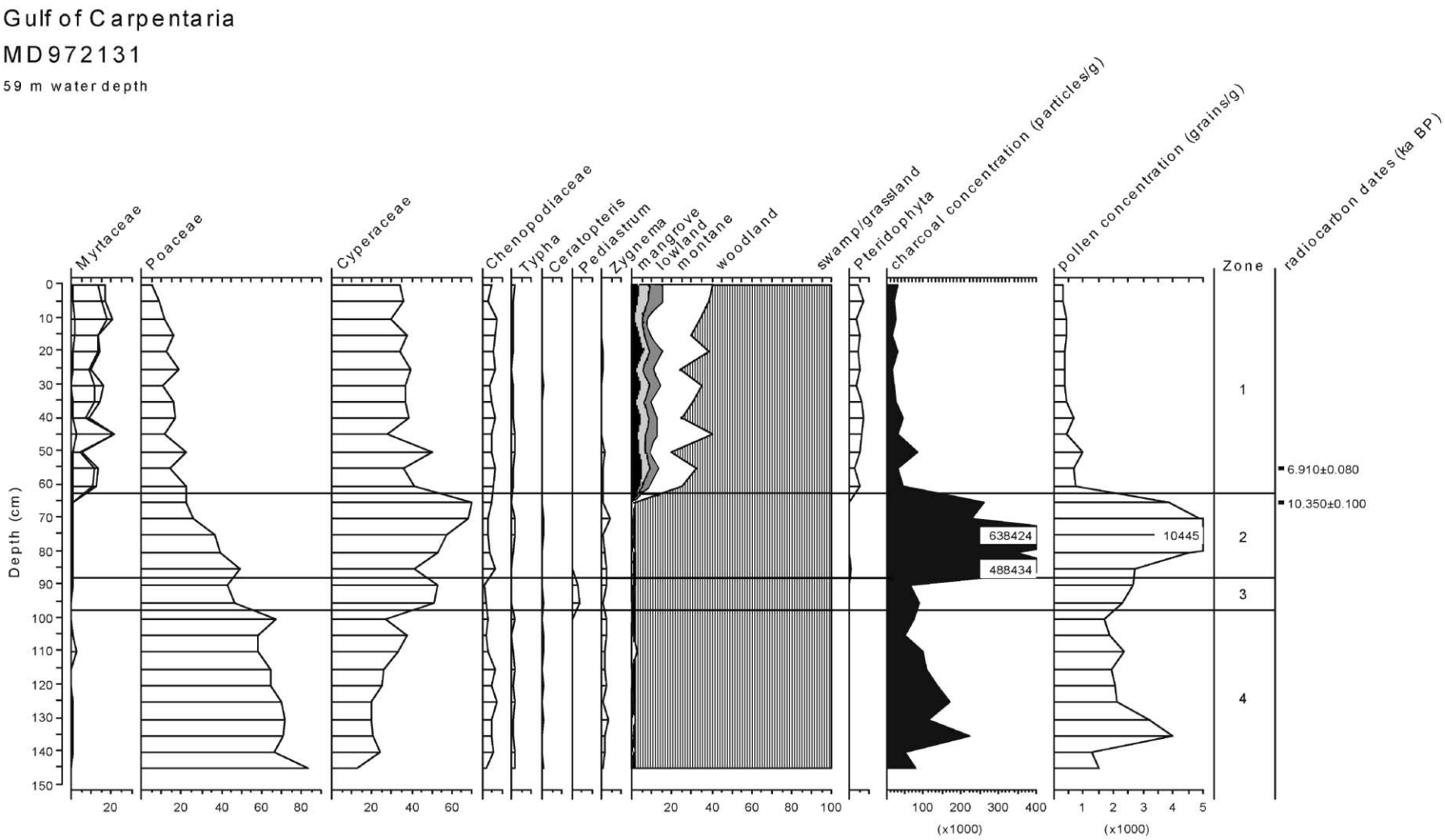


Fig. 15. Summary pollen diagram for the upper 150 cm of core MD-31 from the Gulf of Carpentaria.

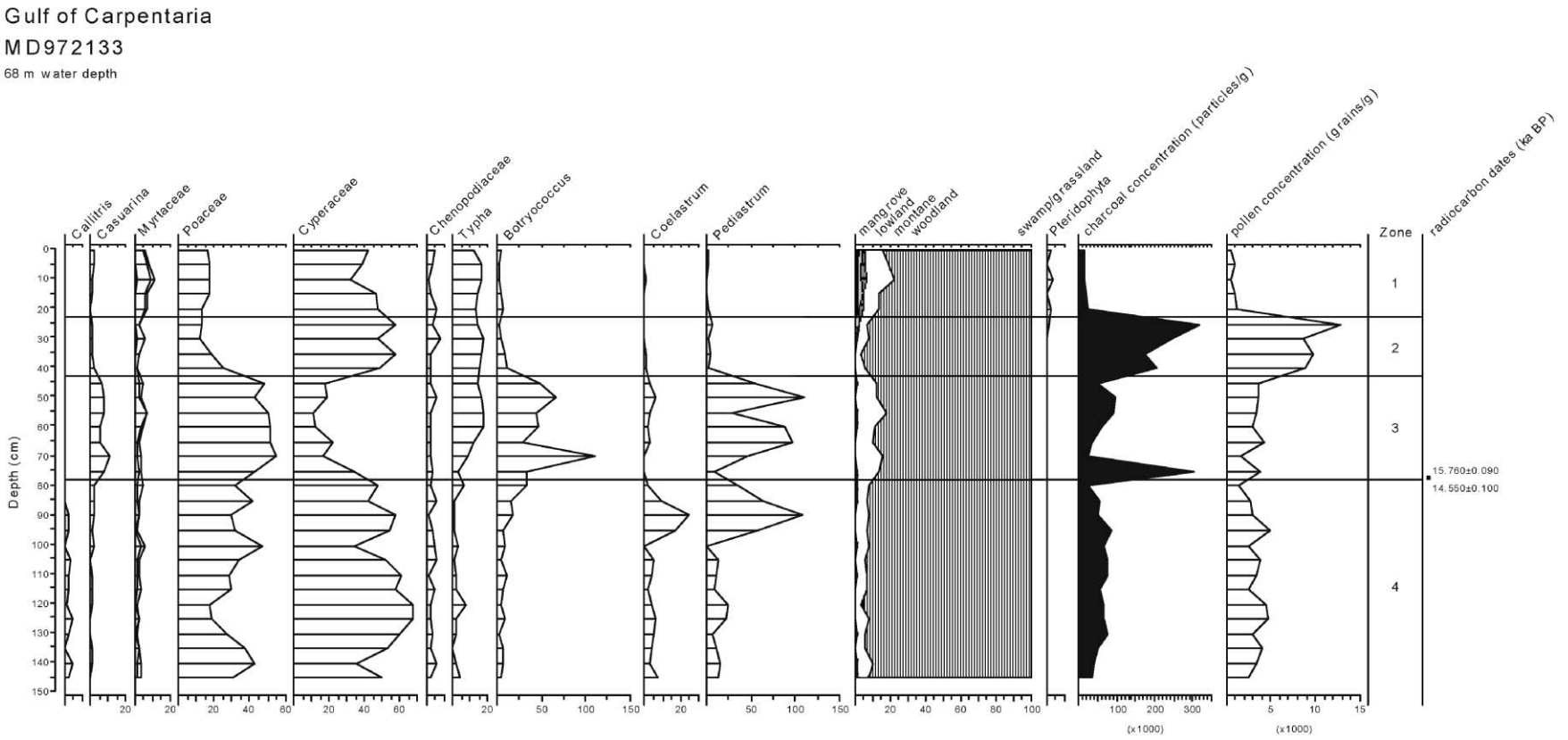


Fig. 16. Summary pollen diagram for the upper 150 cm of core MD-33 from the Gulf of Carpentaria.

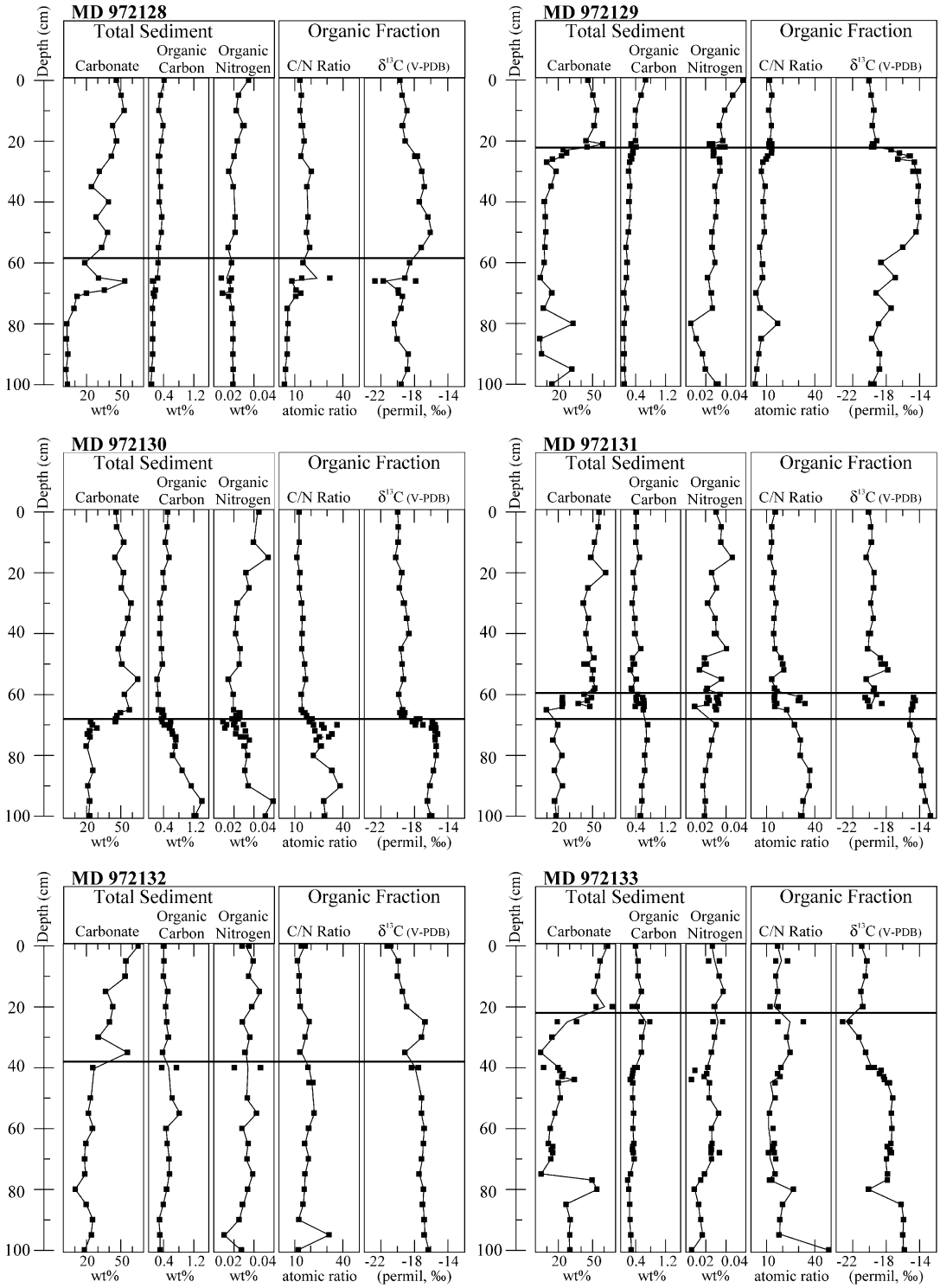


Fig. 17. Total carbonate content, organic carbon content, organic nitrogen content, atomic C/N ratio, and $\delta^{13}C$ values of organic matter for the top metre of all six MD cores, Gulf of Carpentaria. The horizontal lines mark the position of the non-marine/marine transition.

Territory, Chivas, 1991; northern Queensland east coast, Torgersen et al., 1983a, Torgersen and Chivas, 1985, Gagan et al., 1987, 1990; Gulf of Papua, Bird et al., 1995).

The core-top sediment samples from MD-28–MD-33 contain bulk organic matter with $\delta^{13}C$ values of –19 to –21‰ (Fig. 17), which is similar to those of the modern marine particulate organic carbon (Rothlisberg

et al., 1994). In the cores from the more westerly side of the Gulf, MD-29–MD-31, there is an abrupt change in the $\delta^{13}C$ values of organic carbon at the marine/non-marine boundary, to values of –14 to –15‰. Such values are typical of terrestrial vegetation with a predominance of $C_4$ grasslands (which have a $\delta^{13}C$ value of –12 to –15‰) over $C_3$ woodland and mangrove vegetation which typically has $\delta^{13}C$ values of –25 to –30‰ (O'Leary, 1988). In cores MD-30 and MD-31, this change is accompanied by an increase in C/N ratios from 10 to 30, which supports the influence of $C_4$ terrestrial vegetation, as the latter typically have C/N ratios greater than 30 (e.g. Meyers, 1994). However, in the other MD cores, the preserved non-marine organic carbon typically has more positive $\delta^{13}C$ values in the range –20 to –16‰, without increased C/N ratios. This is more difficult to explain with respect to the currently characterised marine/non-marine $^{13}C$ and C/N end-members (Meyers, 1994), although the presence of aquatic and algal organic detritus, rather than the remains of terrestrial vascular plants, is implied. A possible solution lies in these non-marine organic carbon components being largely derived from lacustrine algae having $\delta^{13}C$ values similar to organic matter from the surrounding watershed, which in this case would have been dominated by $C_4$ grasses. A clearer resolution awaits the determination of $\delta^{13}C$ of the calcareous fossils from the non-marine facies which will provide an estimate of the $\delta^{13}C$ value of the non-marine dissolved bicarbonate.

## 5. Synthesis

The base of the longest core, MD-32, has been dated at about 125 ka by TL and OSL methods, with supporting ages on molluscs a little higher in the core from AAR dating. The basal unit is an iron-mottled sand with evidence of sub-aerial exposure overlain at 14.1 m by dark grey marine silty clay. This is interpreted as the Marine Isotopic Stage 6/5 marine transgression, which has a duration from 128 to 116 ka (Stirling et al., 1998). Thus we interpret the base of core MD-32 as having an age nearer 130 ka (or slightly greater), which is well within the error estimates of the available dates.

The sea-level curve derived from $\delta^{18}O$ values of marine benthic Foraminifera (Shackleton, 1987) and independently determined sea-levels (filled circles) from survey and dating of the uplifted coral terraces of the Huon Peninsula, Papua New Guinea (Chappell et al., 1996) is shown in Fig. 18. Two horizontal lines placed at –50 and –60 m are indicative of the height of the Arafura Sill, although this will not necessarily have remained constant through time, especially as the effects of hydro-isostasy and rebound have not been taken into account. Thus, the anticipated sedimentary facies in core MD-32, as related to this sea-level curve, would be largely marine in the lower parts, overlain by non-marine units and separated by several possible minor transgressions and regressions during the interval 80–40 ka. This broadly matches the sediment facies variations seen in the available cores, although the details of the oscillations in the 80–40 ka period await independent dating.

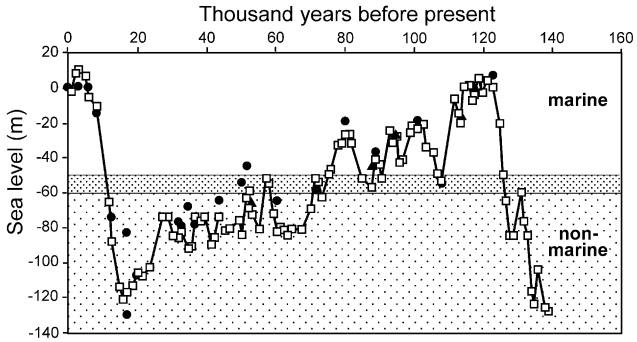


Fig. 18. Global sea-level curve for the past 140 ka derived from $\delta^{18}O$ values of benthic foraminifers (Shackleton, 1987), with selected data (filled circles) from the surveyed coral terraces at the Huon Peninsula (Chappell et al., 1996). The horizontal lines at –50 and –60 m are indicative of the depth of the Arafura Sill, and the labels "marine" and "non-marine" indicate the environments pertaining to the Gulf of Carpentaria/Lake Carpentaria.

The younger Marine Isotopic Stage 2/1 marine transgression (at approximately 9.7 ka) is reasonably well understood, as are the palaeoenvironments of the lacustrine phase before this transgression. A number of techniques (e.g. palynology, assemblages of foraminifers and ostracods, $\delta^{13}C$ and C/N of organic matter) permit the definition of both aquatic and terrestrial environments, and support the existence of savanna grassland at this time, with no evidence of dense jungle lowland, such as is presently found, for example, in southern Papua. Several lines of evidence (the presence and position of palaeo-exposure surfaces, palynology and carbonate microfossil assemblages) support a Lake Carpentaria that expanded to near lake-full conditions prior to the 9.7 ka marine transgression.

## Acknowledgements

We thank the scientific and logistic crews of the *Marion Dufresne* and their leader Yvon Balut. Those persons who participated in the cruise (Luc Beaufort as cruise chief scientist, Allan Chivas, Martine Couapel, Frank Dulong, Terry Edgar and Adriana García) learned much during their involvement with such a professional team. We also acknowledge those who helped to organise the cruise, including Jean-Louis

Turon and Elizabeth Michel and for support from the IMAGES program from Laurent Labeyrie and Franck Bassinot. The continuing work in the Gulf of Carpentaria represents a long-term collaboration among the University of Wollongong, the Australian National University and the US Geological Survey.

We gratefully acknowledge the support provided by Sophie Bieda (core dissection, CEREGE), Geoff Black (transport of cores), Richard Miller (cartography), David Carrie (X-ray diffraction), John Reid and John Marthick (computing), Michelle Baker, Julia Bailey and Louisa Willdin (manuscript preparation), and G.J. Broadbent and Ray Peddersen from Queensland Transport (Marine Division) for tidal data. Sandrine Pendu, Université de Paris XI, Orsay, assisted with sample preparation during a six-month magistère program in Wollongong.

The $^{14}C$ dating was supported by grant 98/155R from the Australian Institute of Nuclear Science and Engineering, and we acknowledge the technical assistance of Quan Hua, Ugo Zoppi, Geraldine Jacobsen and other members of the ANSTO AMS Centre. The Faculty of Engineering at the University of Wollongong provided access to the particle-size analyser. The project was largely funded by the Australian Research Council (grant A39600498) and by the Quaternary Environments Research Centre, the University of Wollongong. We thank John Head for helpful discussion on several aspects of the work. We appreciate the reviews of the manuscript provided by Bob Carter and an anonymous referee. This paper is a contribution to the International Geological Correlation Program (IGCP) projects, 396 and 464 on Continental Shelves in the Quaternary.

## Appendix A. 1997 Coring

Almost 10 tonnes of lead weights were used to impale the piston corer, and the relatively poor penetration (compared to 40–60 m in open marine oozes, using the same system) is a result of the semi-lithified nature of the Gulf sediments, with their common calcretised and ferruginous intervals. The retrieved cores were sectioned on-board to 1.5 m lengths, passed through a MST (multi-sensor track recorder) for magnetic susceptibility, *P*-wave velocity and $\gamma$-ray density measurements; split longitudinally and subject to digital photography and digital and Munsell colour measurement; and preliminary core description. The cores were maintained at 4°C aboard the ship. Five of the six cores were landed at Weipa where they were also maintained at 4°C, before a short flight to Brisbane and into another cool room, thence another flight to the Sydney airport coolroom, and finally by road to a 4°C laboratory at the University of Wollongong. The sixth core (MD972132), an IMAGES reference core, was returned to France, to a 4°C container at CEREGE, Aix-en-Provence, before detailed sampling and return of half the core, in segmented form, to Wollongong in February 2000.

## Appendix B. Segmentation of the 1997 cores

One split half of each core was logged in the cool laboratory, and sliced into 1-cm depth-interval segments, that were weighed and stored flat in transparent glass Petri dishes with tape-sealed lids. Individual 1-cm samples from every 5-cm depth increment (see Fig. 19) were further dissected for a variety of purposes, including palynology, micropalaeontology, nannofossils, diatoms, sedimentology (particle-size, XRD mineralogy, $H_2O$, organic matter and $CaCO_3$ contents), and bulk geochemistry. About one third of the volume of each of these slices was retained in the Petri dishes for later use and/or archiving. The dissection of five of the cores occurred in a 4°C laboratory in Wollongong. The sixth core was similarly dissected at CEREGE, not under cool-room conditions but with individual core lengths of 1.5 m removed from a 4°C store and segmented within a single day.

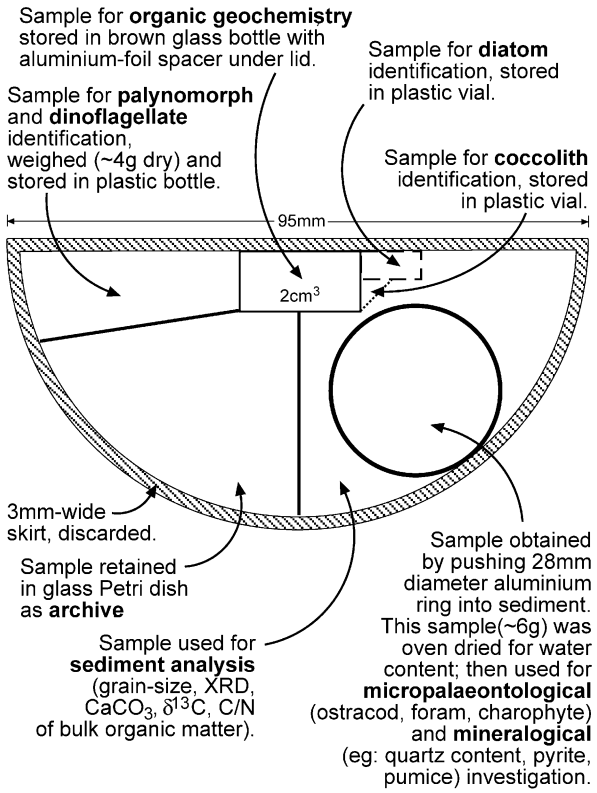


Fig. 19. Scheme for segmentation of a 1-cm thick slice of split core that shows the various subsamples, their storage, and analysis.

Our strategy of segmenting and sub-sampling the core was designed to produce 1-cm depth-increment samples for most types of investigations, with equivalent and comparable sub-samples, each appropriately handled and stored (notionally, in perpetuity at 4°C), without the need for disruptive sequential re-sampling of core. The horizontal segmentation of the core also produced a large surface area for inspection (95.3 $cm^2$ per cm of depth-increment) compared to that of the exposed surface of split core (9.5 $cm^2$ per cm of depth-increment), and this greatly facilitated visual core logging of facies, and 'discovery' of fossils, calcrete nodules, etc., not exposed in the working face of the split core. Thus from 53.68 linear metres of core, from six coring sites, there are 5368 individually stored segments of which approximately 1050 segments (i.e. every fifth single-centimetre slice) were further prepared for the investigations reported here.

## Appendix C. Particle-size analysis

Sediment particle-size analysis was performed on 1030 samples of untreated sediment from all MD cores using a Malvern Mastersizer 2600. This instrument permits rapid analysis of particle size using the principles of laser obscuration. Subsamples taken across the full 1-cm depth interval of each sample aliquot were dispersed in the sample preparation bath by both physical and ultrasonic agitation. Agitation continued until a stable particle-size distribution was observed and the obscuration level had stabilised. The sample was then analysed using the polydispersive mode calculated over one experiment, with results calculated on 10,000 sweeps.

The sand fraction ($>63$ μm) in all cores represents less than 20% of the particle-size distribution. Observation of subsamples from cores MD-31 and MD-32 with a binocular microscope, revealed that the sand fraction is composed of sub-angular to sub-rounded quartz and minor lithic fragments, pyrite spherules and framboids, recrystallised and recalcified carbonate microfossils (commonly almost entirely *Ammonia* spp.), and ferruginised material including echinoderm fragments. The abundant more fragile shell fragments identified in several samples prior to processing were probably destroyed by agitation during particle-size analysis.

Since the sediment samples were not reacted with acid prior to particle-size determination, some of the measured sand-sized material could be due to the presence of more mechanically resistant calcareous microfossils. However, the abundance of the sand-sized fraction is low throughout, and not particularly high in horizons where microfossils are more abundant. Some of the isolated higher abundances of sand, particularly in deeper portions of the cores correspond to the presence of pedogenic carbonate nodules.

## Appendix D. Amino acid racemisation dating

After pretreatment cleaning procedures using dental tools and successive dilute acid etches, whole valves were digested in 8 M HCl, followed by hydrolysis, cation-exchange separation of residual protein and derivatization. Analyses of the N-pentafluoropropionyl D, L-amino acid 2-propyl esters were undertaken using a Hewlett-Packard 5890A Series II gas chromatograph with a flame ionisation detector and a 25 m coiled fused silica capillary column coated with the stationary phase Chirasil-L-Val. In this work, the extent of racemisation is reported for the enantiomeric amino acids aspartic acid (ASP), glutamic acid (GLU), leucine (LEU) and valine (VAL).

With the exception of GLU, the extent of racemisation of the different amino acids in each mollusc is consistent with established relative rates of racemisation in Quaternary molluscs ($VAL \leqslant LEU < ASP$: Lajoie et al., 1980; Murray-Wallace et al., 1988). GLU, however, showed a higher degree of racemisation than aspartic acid, a result which may relate to the crossing-over phenomenon reported by Lajoie et al. (1980), whereby in late diagenesis the kinetic pathway for one amino acid may intersect the pathway of another amino acid, yielding an apparent reversal in extent of racemisation.

A high degree of racemisation of amino acids was determined in the fossil molluscs, particularly for GLU which is close to equilibrium for the molluscs from the basal portion of the core (Table 3). A comparable extent of racemisation is apparent for the *Anadara* (UWGA-551) and *Bassina* (UWGA-550) specimens suggesting a similar age for these fossil molluscs. In contrast, the *Bassina* specimen (UWGA-548) from 5.00 to 5.02 m is significantly younger. By analogy with more extensive racemisation data from southern Australia (Murray-Wallace, 1995), and making due allowance for the significantly higher diagenetic temperatures for the molluscs from the Gulf of Carpentaria, the extent of racemisation points to a Late Pleistocene age. The extent of racemisation in a Holocene radiocarbon calibrated specimen of *Anadara* (*Tegillarca*) *granosa* from Princess Charlotte Bay, Queensland, also reveals that the Gulf of Carpentaria fossils are significantly older than Holocene (Table 3). Current mean annual air temperature at Princess Charlotte Bay and Gulf of Carpentaria is 26°C, which highlights the appropriateness of the calibration used.

Conversion of the enantiomeric ratios to numeric ages is more problematic and requires either direct calibration by another dating method, such as radiocarbon on a specimen also analysed by AAR, or a knowledge of the diagenetic temperature history. In this work, preliminary ages are assigned to the fossil molluscs by calibrating the results obtained here with results for a

Table 3
Extent of amino acid racemisation (total acid hydrolysate) in marine molluscs from Gulf of Carpentaria core MD972132

| Species | Depth in core (m) | Lab code or reference | Amino acid D/L ratio[a] | | | | Numeric age (ka) |
|---|---|---|---|---|---|---|---|
| | | | VAL | LEU | ASP | GLU | |
| *Bassina* sp. (disarticulated) | 5.00–5.02 | UWGA-548 | 0.531±0.005 | 0.539±0.002 | 0.519±0.014 | 0.614±0.015 | 72±11 |
| *Bassina* sp. (articulated) | 12.38–12.40 | UWGA-550 | 0.688±0.013 | 0.724±0.015 | 0.815±0.002 | 0.977±0.007 | 122±18 |
| *Anadara (Tegillarca) granosa* (articulated) | 13.18–13.19 | UWGA-551 | 0.649±0.017 | 0.653±0.001 | 0.611±0.088 | 0.925±0.012 | 108±16 |
| *Anadara (Tegillarca) granosa* | 4.61(PCB#1) | Murray-Wallace and Kimber (1988) | 0.171±0.006 | 0.287±0.005 | — | — | 7.43±0.13[b] |

[a] Amino acids: VAL, valine; LEU, leucine; ASP, aspartic acid and GLU, glutamic acid.
[b] As determined by radiocarbon dating.

previously published sample from Princess Charlotte Bay, which yielded a valine D/L ratio of 0.171±0.006 on a specimen of *Anadara* (*Tegillarca*) *granosa*. The fossil from a vibracore (PCB#1) was buried 4.61 m below the ground surface and has a radiocarbon age (sidereal years) of 7430±130 a cal BP (Murray-Wallace and Kimber, 1988). Use of a kinetic model based on apparent parabolic kinetics (Mitterer and Kriausakul, 1989) with the Holocene calibration sample yielded numeric ages equating with Stage 5 *sensu lato* of the marine oxygen isotope record (Bassinot et al., 1994; Table 3).

The age uncertainty terms account for a 1°C uncertainty in diagenetic temperature. *Anadara (Tegillarca) granosa*, like *Anadara trapezia*, is a shallow-burrowing bivalve of semi-infaunal habit (Murray-Wallace et al., 2000) and *Bassina* sp. frequents a similar habitat. Accordingly, the articulated bivalves reflect minimal *post-mortem* transport and therefore suggest that sedimentation is broadly contemporaneous with the ages derived for these fossils.

## Appendix E. Luminescence dating

Both TL and OSL determinations were made on a single sample (MD-32, 1482 cm) from the base of core MD-32. All sample preparation was carried out in subdued red/orange lights in the OSL Laboratory at the University of Wollongong. A 4-mm layer was removed from each surface of sample MD-32 1482 cm to avoid any sample grains which could have been exposed to daylight. Coarse (106–150 μm and 63–106 μm) quartz grains were extracted for luminescence analyses. The 106–150 μm size fraction was used for OSL analyses, whereas TL measurements were performed on the 63–106 μm grain-size fraction (Table 4). Both grain-size fractions were treated with 8% hydrochloric acid and 30% hydrogen peroxide to remove carbonates and organic materials, respectively. They were then etched in 40% HF for 40 min OSL or 10 min TL to avoid any feldspar contamination in the sample, and to remove the outer alpha-irradiated layer. This was followed by a treatment with hydrochloric acid to remove acid-soluble fluorides. The purity of the quartz extract was checked using infrared stimulated luminescence. All sample aliquots (diameter ~2 mm) were mounted onto 9.7 mm stainless steel discs using silicone oil spray.

### *E.1. Dosimetry*

The dose-rate for this sample was estimated using thick-source alpha-counting (Aitken, 1998) and atomic absorption spectrophotometry. The cosmic-ray dose-rate was calculated using Prescott and Hutton (1988, 1994); an average sample depth of 7.4 m and a sample density of 2 g cm$^{-3}$ was assumed in this calculation. The water content was assumed to be 20±5% for the sample. The dose-rate components were estimated from the alpha count-rates and the potassium concentration using the conversion data given by Aitken (1998). The dose-rate used in estimating the TL age includes a small alpha component as the HF etching time was limited to 10 min.

### *E.2. Thermoluminescence measurements and results*

All TL measurements were performed on a Littlemore manual TL reader. The optics channel comprised a EMI 9635QB photomultiplier tube coupled to a Corning 7–59 (320–440 nm) transmission filter. Sample aliquots were irradiated using a Littlemore Automatic Irradiator fitted with a $^{90}$Sr/$^{90}$Y plaque beta source. The TL equivalent dose was estimated using a modified regenerative and additive-dose technique (Shepherd and Price, 1990). Fourteen sample aliquots were bleached for 24 h with an

Table 4
Luminescence and radioactivity data for sample MD-972132, 1482-1483 cm[a]

| Grain-size (μm) | TL equivalent dose (Gy) | OSL equivalent dose (Gy) | Alpha-counting | | AAS[b] potassium (wt%) | Dose-rate[c] ($mGy\,a^{-1}$) | TL age (ka) | OSL age (ka) |
|---|---|---|---|---|---|---|---|---|
| | | | Thorium (ppm) | Uranium (ppm) | | | | |
| 106–150 | — | 246±15 | 10±0.5 | 3.1±0.06 | 0.9±0.02 | 2.0±0.14 | — | 125±12 |
| 63–106 | 260±33 | — | 10±0.5 | 3.1±0.06 | 0.9±0.02 | 2.1±0.16 | 123±16 | — |

[a] Note that the Th, U and K contents were measured on an aliquot of the bulk sample before its disaggregation to separate the several quartz fractions.
[b] AAS = Atomic absorption spectrophotometry.
[c] Water content (assumed) = 20±5%; the measured water-content at the time of sample preparation was 19.5%.

UV lamp (Phillips MLU 300W) and then given various doses to construct a regeneration TL growth curve. The mean of eight natural TL measurements was interpolated into the regeneration growth curve to determine the equivalent dose. Another six aliquots were used to confirm the absence of sensitivity changes in the sample during laboratory procedures. A third-order polynomial was used for fitting the regeneration TL growth curve. The TL equivalent dose was estimated to be 260±33 Gy. As the total dose-rate is $\sim 2.11\,mGy\,a^{-1}$, the TL age is estimated to be 123±16 ka.

### *E.3. Optically stimulated luminescence measurements*

An automated Risø TL/OSL reader (Bøtter-Jensen et al., 1999) fitted with a broad-band, blue–green stimulation source (420–550 nm) and three U-340 detection filters (290–370 nm) was used for OSL measurements. This reader is also equipped with a 40 mCi $^{90}Sr/^{90}Y$ beta source delivering about $0.04\,Gy\,s^{-1}$ for irradiation. All OSL measurements were performed for 40 s at 125°C. The OSL signal used for equivalent dose estimation is the background-corrected 0–1.6 s OSL signal. The equivalent dose for this sample was estimated using the single-aliquot regenerative-dose protocol (see Murray and Wintle, 2000; Banerjee et al., 2000). In this protocol, a natural aliquot is first preheated at some arbitrary temperature (between 160°C and 320°C) for 10 s. This aliquot is then stimulated at 125°C to measure the natural OSL ($L_o$). A test dose is applied ($\leqslant$100% of the natural dose) and the aliquot is heated to 160°C to evict charge from shallow traps (e.g. the 110°C trap in quartz). The OSL signal is measured again, to give $T_o$. Next, a regeneration dose $D_1$ is applied, followed by preheating and measurement of the regenerated OSL ($L_1$). The test dose is given again, heated to 160°C and the OSL signal measured to give $T_1$. The regenerated OSL signals from a second ($L_2$) and a third regeneration dose ($L_3$) and the respective test dose signals ($T_2$ and $T_3$) are then measured in a similar way. A fourth regeneration dose (equal to the first regeneration dose) is given to the aliquot, followed by preheating and subsequent measurement of the regenerated $L_4$ and the test dose signals $T_4$. The sensitivity-corrected regenerated signals ($L_i/T_i, i = 1, ..., 3$) are used to construct a growth curve; the sensitivity-corrected natural ($L_N/T_N$) signal is then interpolated onto the growth curve to obtain an estimate of the equivalent dose.

A ratio of the fourth and the first corrected regenerated OSL signals of close to one confirms that dividing by the test dose response has successfully corrected for changes in the luminescence sensitivity of the sample aliquot. Finally, after measurement of $T_4$, the measurement cycle is repeated with $D_5 = 0$ Gy. The sensitivity-corrected zero-dose signal indicates the extent of thermal assisted recuperation in the sample.

## Appendix F. Micropalaeontological preparation

Micropalaeontological analysis, at 10 cm intervals, is reported for the top metre of cores MD-28 and MD-31, thereby spanning the Holocene marine transgression. Both cores are located approximately mid-way between basin-rim and depocentre. Special care was taken to avoid metal contamination during sample processing to permit later geochemical analysis of the carbonate microfossils. The sediment subsamples for micropalaeontological study (Fig. 19) were oven dried at 40–60°C in 250 ml glass jars and the attendant weight loss provided the water content displayed in the last column of Figs. 4–9. After drying, the jar was filled with deionised water and the sediment left to disaggregate for at least 15 h. The sediment was wet-sieved with deionised water through 63 μm nylon mesh in plastic sieve-support rings, the coarse fraction dried at 40–50°C, and stored in glass bottles (to avoid static electricity) with plastic caps. Aliquots of sediment were prepared for assemblage analysis using a microsplitter. A minimum of 300 foraminifers, all ostracods and charophytes, representatives of other biological remains (molluscs, echinoderms, pteropods), and mineral grains (quartz, glauconite), were separated and examined. The analysis of the biotic and abiotic content of the samples allowed the recognition of biocoenosis/thanatocoenosis,

and type/degree of transportation, providing data for palaeoenvironmental reconstruction. The identification of the microfossils was made using a variety of sources, including Loeblich and Tappan (1987, 1994), Murray (1991), and Yassini et al. (1993).

## Appendix G. Palynological sample preparation

Weighed samples of approximately 4 $cm^3$ were processed as follows: 10% sodium pyrophosphate; 210 μm sieving; sieving over a 7 μm screen; 10% HCl; acetolysis (10 min); heavy liquid separation (sodium polytungstate S.G. 2.0, 20 min at 2000 rpm) (3 ×); 40% HF; ethanol; glycerol. A known amount of *Lycopodium* spores was added to the samples prior to processing to allow calculation of pollen and charcoal concentrations. Slides were mounted with glycerol and sealed with paraffin wax. The slides were counted along evenly spaced transects on a Zeiss Axioskop microscope with Plan-Apochromat 63 ×/1.40 oil DIC and Plan-NeoFluar 100 ×/1.30 oil DIC objectives. The minimum pollen sum on which all percentages were calculated, was approximately 200 pollen grains. Total pollen concentrations (grains/g) and charcoal concentrations (particles/g) are expressed per gram of dry sediment using the moisture content measured on another sediment aliquot from the same depth interval (Fig. 19). In core MD-29, the interval between 85 and 150 cm was nearly devoid of pollen, almost certainly as a result of an intense pedogenic overprint.

## Appendix H. Geochemical methods

Individual samples, commonly from 5 cm intervals, but at 1 cm intervals at some transitions, were oven dried at 60°C (= $H_2O$ content), acidified with 1 M HCl (weight loss attributed to $CaCO_3$), and combusted in a Carlo Erba NA 1500 NCS elemental analyser (thermal conductivity detector = C% and N%) on-line with a Micromass PRISM III continuous-flow triple-collector mass spectrometer, for $\delta^{13}C$ measurement of the combustion $CO_2$.

## References


Aitken, M.J., 1998. An Introduction to Optical Dating. Oxford University Press, Oxford and New York, 267pp.

Banerjee, D., Bøtter-Jensen, L., Murray, A.S., 2000. Estimation of the quartz equivalent dose in retrospective dosimetry using the single-aliquot regenerative-dose protocol. Applied Radiation and Isotopes 52, 831–844.

Bard, E., Arnold, M., Hamelin, B., Tisnerat-Laborde, N., Cabioch, G., 1998. Radiocarbon calibration by means of mass spectrometric $^{230}Th/^{234}U$ and $^{14}C$ ages of corals. An updated data base including samples from Barbados, Mururoa and Tahiti. Radiocarbon 40, 1085–1092.

Bassinot, F.C., Labeyrie, L.D., Vincent, E., Quidelleur, X., Shackleton, N.J., Lancelot, Y., 1994. The astronomical theory of climate and the age of the Brunhes-Matuyama magnetic reversal. Earth and Planetary Science Letters 126, 91–108.

Bird, M.I., Brunskill, G.J., Chivas, A.R., 1995. Carbon-isotope composition of sediments from the Gulf of Papua. Geo-Marine Letters 15, 153–159.

Blake, T., Burgess, I.R., Stewart, O.C., Low, E., 1984. Duyken-1 well completion report. Permit NT/P30, Carpentaria Basin, Northern Territory, Australia. Canada Northwest Australia Oil N.L. (held as Northern Territory Geological Survey, unpublished Report PR85/31B; and as AGSO unpublished Report 84/577).

Bøtter-Jensen, L., Duller, G.A.T., Murray, A.S., Banerjee, D., 1999. Blue light emitting diodes for optical stimulation of quartz in retrospective dosimetry and dating. Radiation Protection Dosimetry 84, 335–340.

Cecil, C.B., 1990. Paleoclimate controls on stratigraphic repetition of chemical and siliciclastic rocks. Geology 18, 533–536.

Cecil, C.B., Stanton, R.W., Neuzil, S.W., Dulong, F.T., Ruppert, L.F., Pierce, B.F., 1985. Paleoclimate controls on late Paleozoic peat formation and sedimentation in the central Appalachian basin (USA). International Journal of Coal Geology 5, 195–230.

Cecil, C.B., Dulong, F.T., Cobb, J.C., Supardi, 1993. Allogenic and autogenic controls on sedimentation in the central Sumatra basin as an analogue for Pennsylvanian coal-bearing strata in the Appalachian basin. In: Cobb, J.C., Cecil, C.B. (Eds.), Modern and Ancient Coal-Forming Environments. Geological Society of America, Special Paper 286, pp. 3–22.

Chappell, J., Omura, A., Esat, T., McCulloch, M., Pandolfi, J., Ota, Y., Pillans, B., 1996. Reconciliation of late Quaternary sea levels derived from coral terraces at Huon Peninsula with deep sea oxygen isotope records. Earth and Planetary Sciences Letters 141, 227–236.

Chivas, A.R., 1991. Isotopic tracers of recent sedimentary environments. Proceedings of the Fourth Edgeworth David Symposium, Department of Geology and Geophysics, University of Sydney, pp. 55–61.

Chivas, A.R., De Deckker, P., Shelley, J.M.G., 1983. Magnesium, strontium, and barium partitioning in non-marine ostracode shells and their use in paleo-environmental reconstructions—a preliminary study. In: Maddocks, R.F. (Ed.), Applications of Ostracoda: Proceedings of the Eighth International Symposium on Ostracodes. University of Houston, Geosciences, pp. 238–249.

Chivas, A.R., De Deckker, P., Shelley, J.M.G., 1985. Strontium content of ostracods indicates lacustrine palaeosalinity. Nature 316, 251–253.

Chivas, A.R., De Deckker, P., Shelley, J.M.G., 1986a. Magnesium content of non-marine ostracod shells: a new palaeosalinometer and palaeothermometer. Palaeogeography, Palaeoclimatology, Palaeoecology 54, 43–61.

Chivas, A.R., De Deckker, P., Shelley, J.M.G., 1986b. Magnesium and strontium in non-marine ostracod shells as indicators of palaeosalinity and palaeotemperature. Hydrobiologia 143, 135–142.

Chivas, A.R., De Deckker, P., Cali, J.A., Chapman, A., Kiss, E., Shelley, J.M.G., 1993. Coupled stable-isotope and trace-element measurements of lacustrine carbonates as paleoclimatic indicators. In: Swart, P.K., Lohmann, K.C., McKenzie, J., Savin, S. (Eds.), Climate Change in Continental Isotopic Records. American Geophysical Union Monograph 78, pp. 113–121.

Church, J.A., Forbes, A.M.G., 1981. Non-linear model of the tides in the Gulf of Carpentaria. Australian Journal of Marine and Freshwater Research 32, 685–697.

Cobb, J.C., Cecil, C.B., 1993. Modern and ancient coal-forming environments. Geological Society of America, Special Paper 286, 1–198.

De Deckker, P., Chivas, A.R., Shelley, J.M.G., Torgersen, T., 1988. Ostracod shell chemistry: a new palaeoenvironmental indicator applied to a regressive/transgressive record from the Gulf of Carpentaria, Australia. Palaeogeography, Palaeoclimatology, Palaeoecology 66, 231–241.

De Deckker, P., Corrège, T., Head, J., 1991. Late Pleistocene record of eolian activity from tropical northeastern Australia suggesting the Younger Dryas is not an unusual climatic event. Geology 19, 602–605.

Edgar, N.T., Cecil, C.B., Grim, M.S., Chappell, J., 1994. Allocyclic stratigraphy beneath the floor of the Gulf of Carpentaria, Northern Australia, based on high-resolution seismic survey. Geological Society of America Abstracts with Programs 26 (7), A–229.

Edgar, N.T., Cecil, C.B., Mattick, R., Chivas, A.R., De Deckker, P., Djajadihardja, Y. A modern analogue for tectonic, eustatic, and climatic processes in cratonic basins: Gulf of Carpentaria, northern Australia. In: Cecil, C.B., Edgar, T.N.(Eds), Allocyclic Controls on Stratigraphy and Sedimentation. Special Publication, Society of Economic Paleontologists and Mineralogists, in press.

Fairbridge, R.W., 1953. The Sahul shelf—northern Australia—its structural and geological relationships. Journal of the Royal Society of Western Australia 37, 1–33.

Gagan, M.K., Sandstrom, M.W., Chivas, A.R., 1987. Restricted terrestrial carbon input to the continental shelf during Cyclone Winifred: implications for terrestrial runoff to the Great Barrier Reef Province. Coral Reefs 6, 113–119.

Gagan, M.K., Chivas, A.R., Herczeg, A.L., 1990. Shelf-wide erosion, deposition, and suspended sediment transport during Cyclone Winifred, central Great Barrier Reef, Australia. Journal of Sedimentary Petrology 60, 456–470.

Grim, M.S., Edgar, N.T., 1998. Bathymetric map of the Gulf of Carpentaria and the Arafura Sea, 1:2,500,000. US Geological Survey, Geologic Investigations Series, map I-2550.

Head, M.J., De Deckker, P., Lawson, E.M., 1999. The use of natural $^{14}C$ as a tracer to identify the incorporation of younger material into the organic component of sediments from the Gulf of Carpentaria, Australia. International Atomic Energy Agency (IAEA) Technical Document 1094. Proceedings Marine Pollution Symposium, Monaco, October 1998. IAEA Vienna, pp. 226–230.

Hill, B.J., 1994. Preface. Ecology of the Gulf of Carpentaria. Australian Journal of Marine and Freshwater Research 45 (3), iii–vii (plus pp. 265–454).

Jones, M.R., 1987. Surficial sediments of the western Gulf of Carpentaria, Australia. Australian Journal of Marine and Freshwater Research 38, 151–167.

Jones, M.R., Torgersen, T., 1988. Late Quaternary evolution of Lake Carpentaria on the Australian–New Guinea continental shelf. Australian Journal of Earth Sciences 35, 313–324.

Lajoie, K.R., Wehmiller, J.F., Kennedy, G.L., 1980. Inter- and intrageneric trends in apparent racemization kinetics of amino acids in Quaternary mollusks. In: Hare, P.E., Hoering, T.C., King, K. (Eds.), Biogeochemistry of Amino Acids. Wiley, New York, pp. 305–340.

Loeblich Jr., A.R., Tappan, H., 1987. Foraminiferal Genera and their Classification, 2 vols. Van Nostrand Reinhold Company, New York, 1182pp.

Loeblich Jr., A.R., Tappan, H., 1994. Foraminifera of the Sahul Shelf and Timor Sea. Cushman Foundation Special Publication 31, 661pp.

Long, B.G., Poiner, I.R., 1994. Infaunal benthic community structure and function in the Gulf of Carpentaria, northern Australia. Australian Journal of Marine and Freshwater Research 45, 293–316.

McCulloch, M.T., De Deckker, P., Chivas, A.R., 1989. Strontium isotope variations in single ostracod valves from the Gulf of Carpentaria, Australia: a palaeoenvironmental indicator. Geochimica et Cosmochimica Acta 53, 1703–1710.

Meyers, P.A., 1994. Preservation of elemental and isotopic source identification of sedimentary organic matter. Chemical Geology 114, 289–302.

Mitterer, R.M., Kriausakul, N., 1989. Calculation of amino acid racemization ages based on apparent parabolic kinetics. Quaternary Science Reviews 8, 353–357.

Murray, A.S., Wintle, A.G., 2000. Luminescence dating of quartz using an improved single-aliquot regenerative-dose protocol. Radiation Measurements 32, 57–73.

Murray, J.W., 1991. Ecology and Palaeoecology of Benthic Foraminifera. Longman Scientific and Technical, New York, 396pp.

Murray-Wallace, C.V., 1993. A review of the application of the amino acid racemisation reaction to archaeological dating. The Artefact 16, 19–26.

Murray-Wallace, C.V., 1995. Aminostratigraphy of Quaternary coastal sequences in southern Australia—an overview. Quaternary International 26, 69–86.

Murray-Wallace, C.V., Kimber, R.W.L., 1988. A review of amino acid racemisation dating and its application to Australian Quaternary marine molluscs—current trends and future prospects. In: Prescott, J.R. (Ed.), Archaeometry: Australasian Studies 1988. Department of Physics and Mathematical Physics, The University of Adelaide, pp. 6–21.

Murray-Wallace, C.V., Kimber, R.W.L., Belperio, A.P., Gostin, V.A., 1988. Aminostratigraphy of the last interglacial in Southern Australia. Search 19, 33–36.

Murray-Wallace, C.V., Beu, A.G., Kendrick, G.W., Brown, L.J., Belperio, A.P., Sherwood, J.E., 2000. Palaeoclimatic implications of the occurrence of the arcoid bivalve *Anadara trapezia* (Deshayes) in the Quaternary of Australasia. Quaternary Science Reviews 19, 559–590.

Nix, H.A., Kalma, J.D., 1972. Climate as a dominant control in the biogeography of northern Australia and New Guinea. In: Walker, D. (Ed.), Bridge and Barrier: the Natural and Cultural History of Torres Strait. Department of Biogeography and Geomorphology, The Australian National University, Canberra, A.C.T., Publ. BG/3, pp. 61–91.

Norman, M.D., De Deckker, P., 1990. Trace metals in lacustrine and marine sediments: a case study from the Gulf of Carpentaria, northern Australia. Chemical Geology 82, 299–318.

O'Leary, M.H., 1988. Carbon isotopes in photosynthesis. Bioscience 38, 328–336.

Passmore, V.L., Williamson, P.E., Gray, A.R.G., Wellman, P., 1993a. The Bamaga Basin—a new exploration target. In: Carman, G.J., Carman, Z. (Eds), Petroleum Exploration and Development in Papua New Guinea. Proceedings of the Second Papua New Guinea Petroleum Convention, Port Moresby, 31 May–2 June 1993, pp. 233–240.

Passmore, V.L., Williamson, P.E., Maung, T.U., Gray, A.R.G., 1993b. The Gulf of Carpentaria—a new basin and new exploration targets. APEA (Australian Petroleum Exploration Association) Journal 33, 297–314.

Phipps, C.V.G., 1966. Gulf of Carpentaria (Northern Australia). In: Fairbridge, R.W. (Ed.), The Encyclopedia of Oceanography (Encyclopedia of Earth Sciences Series, Vol. 1). Reinhold, New York, pp. 316–324.

Phipps, C.V.G., 1970. Dating of eustatic events from cores taken in the Gulf of Carpentaria and samples from the New South Wales continental shelf. Australian Journal of Science 32, 329–331.

Phipps, C.V.G., 1980. The Carpentaria plains. In: Henderson, R.A., Stephenson, P.J. (Eds.), The Geology and Geophysics of

Northeastern Australia. Geological Society of Australia, Queensland Division, pp. 382–386, 388–390.

Prescott, J.R., Hutton, J.T., 1988. Cosmic ray and gamma ray dosimetry for TL and ESR. Nuclear Tracks and Radiation Measurements 14, 223–227.

Prescott, J.R., Hutton, J.T., 1994. Cosmic ray contributions to dose-rates for luminescence and ESR dating: large depths and long-term time variations. Radiation Measurements 23, 497–500.

Rothlisberg, P.C., Pollard, P.C., Nichols, P.D., Moriarty, D.J.W., Forbes, A.M.G., Jackson, C.J., Vaudrey, D., 1994. Phytoplankton community structure and productivity in relation to the hydrological regime of the Gulf of Carpentaria, Australia, in summer. Australian Journal of Marine and Freshwater Research 45, 265–282.

Shackleton, N.J., 1987. Oxygen isotopes, ice volume and sea level. Quaternary Science Reviews 6, 183–190.

Shepherd, M.J., Price, D.M., 1990. Thermoluminescence dating of Late Quaternary dune sand, Manawata/Horowhenua area, New Zealand: a comparison with $^{14}C$ age determinations. New Zealand Journal of Geology and Geophysics 33, 535–539.

Smart, J., 1977. Late Quaternary sea-level changes, Gulf of Carpentaria, Australia. Geology 5, 755–759.

Smart, J., Grimes, K.G., Doutch, H.F., Pinchin, J., 1980. The Carpentaria and Karumba Basins, North Queensland. Australia, Bureau of Mineral Resources, Geology and Geophysics, Bulletin 202, 73pp.

Somers, I.F., Long, B.G., 1994. Note on the sediments and hydrology of the Gulf of Carpentaria, Australia. Australian Journal of Marine and Freshwater Research 45, 283–291.

Stirling, C.H., Esat, T.M., Lambeck, K., McCulloch, M.T., 1998. Timing and duration of the last interglacial: evidence for a restricted interval of widespread coral reef growth. Earth and Planetary Science Letters 160, 745–762.

Stuiver, M., Reimer, P.J., 1993. Extended $^{14}C$ data base and revised CALIB 3.0 $^{14}C$ age calibration program. Radiocarbon 35, 215–230.

Torgersen, T., Chivas, A.R., 1985. Terrestrial organic carbon in marine sediment: a preliminary balance for a mangrove environment derived from $\delta^{13}C$. Chemical Geology (Isotope Geoscience Section) 52, 379–390.

Torgersen, T., Chivas, A.R., Chapman, A., 1983a. Chemical and isotopic characterisation and sedimentation rates in Princess Charlotte Bay, Queensland. BMR (Bureau of Mineral Resources) Journal of Australian Geology and Geophysics 8, 191–200.

Torgersen, T., Hutchinson, M.F., Searle, D.E., Nix, H.A., 1983b. General bathymetry of the Gulf of Carpentaria and the Quaternary physiography of Lake Carpentaria. Palaeogeography, Palaeoclimatology, Palaeoecology 41, 207–225.

Torgersen, T., Jones, M.R., Stephens, A.W., Searle, D.E., Ullman, W.J., 1985. Late Quaternary hydrological changes in the Gulf of Carpentaria. Nature 313, 785–787.

Torgersen, T., Luly, J., De Deckker, P., Jones, M.R., Searle, D.E., Chivas, A.R., Ullman, W.J., 1988. Late Quaternary environments of the Carpentaria Basin, Australia. Palaeogeography, Palaeoclimatology, Palaeoecology 67, 245–261.

Vengosh, A., Kolodny, Y., Starinsky, A., Chivas, A.R., McCulloch, M.T., 1991. Coprecipitation and isotopic fractionation of boron in modern biogenic carbonates. Geochimica et Cosmochimica Acta 55, 2901–2910.

Wintle, A.G., Huntley, D.J., 1979. Thermoluminescence dating of a deep-sea ocean core. Nature 279, 710–712.

Wolanski, E., 1993. Water circulation in the Gulf of Carpentaria. Journal of Marine Systems 4, 401–420.

Yassini, I., Jones, B.G., Jones, M.R., 1993. Ostracods from the Gulf of Carpentaria, northeastern Australia. Senckenbergiana Lethaea 73, 375–406.